

ORNL/TM-13073

ornl

OAK RIDGE
NATIONAL
LABORATORY

MARTIN MARIETTA

RECEIVED

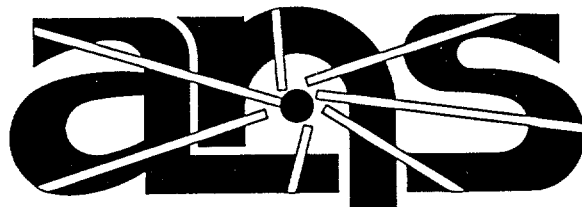
FEB 27 1996

O S T ,

General Purpose
Photoneutron Production
in MCNP4A

F. X. Gallmeier

August 1995



Advanced Neutron Source

DISTRIBUTION OF THIS DOCUMENT IS UNLIMITED *JL*

MANAGED BY
MARTIN MARIETTA ENERGY SYSTEMS, INC.
FOR THE UNITED STATES
DEPARTMENT OF ENERGY

MASTER

This report has been reproduced directly from the best available copy.

Available to DOE and DOE contractors from the Office of Scientific and Technical Information, P.O. Box 62, Oak Ridge, TN 37831; prices available from (615) 576-8401, FTS 626-8401.

Available to the public from the National Technical Information Service, U.S. Department of Commerce, 5285 Port Royal Rd., Springfield, VA 22161.

This report was prepared as an account of work sponsored by an agency of the United States Government. Neither the United States Government nor any agency thereof, nor any of their employees, makes any warranty, express or implied, or assumes any legal liability or responsibility for the accuracy, completeness, or usefulness of any information, apparatus, product, or process disclosed, or represents that its use would not infringe privately owned rights. Reference herein to any specific commercial product, process, or service by trade name, trademark, manufacturer, or otherwise, does not necessarily constitute or imply its endorsement, recommendation, or favoring by the United States Government or any agency thereof. The views and opinions of authors expressed herein do not necessarily state or reflect those of the United States Government or any agency thereof.

ORNL/TM-13073

Computational Physics and Engineering Division

General Purpose Photoneutron Production in MCNP4A

F. X. Gallmeier

August 1995

Prepared by the
OAK RIDGE NATIONAL LABORATORY
Oak Ridge, Tennessee 37831
operated by
LOCKHEED MARTIN ENERGY SYSTEMS, INC.
for the
U.S. DEPARTMENT OF ENERGY
under Contract No. DE-AC05-84OR21400

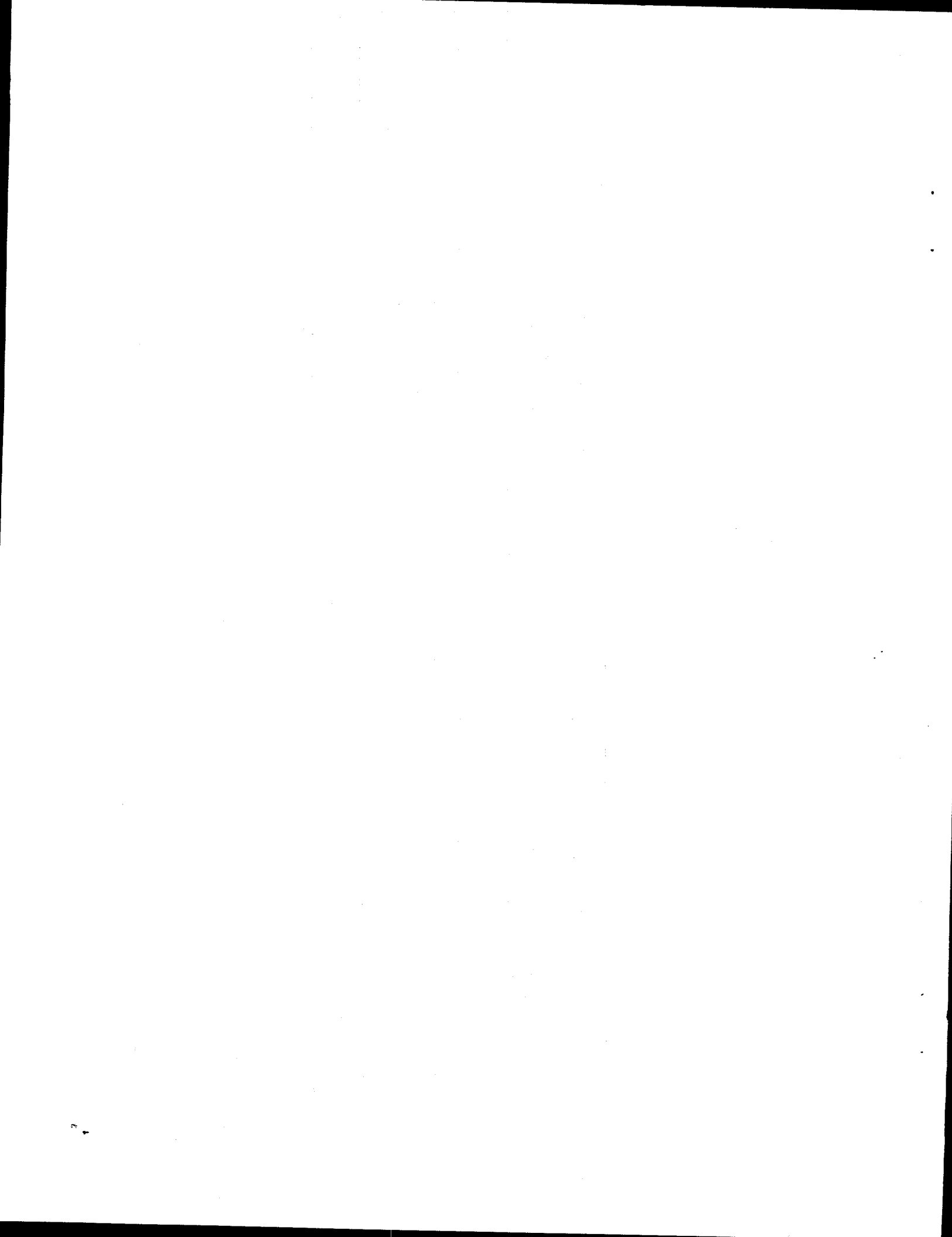
CONTENTS

	Page
LIST OF TABLES	v
LIST OF FIGURES	vii
NOMENCLATURE	ix
ABSTRACT	xi
1. INTRODUCTION	1
2. THE PHOTODISINTEGRATION REACTION	3
2.1 PHOTONEUTRON PRODUCTION CROSS SECTION OF DEUTERIUM	4
2.2 PHOTONEUTRON PRODUCTION CROSS SECTION OF BERYLLIUM	7
3. IMPLEMENTATION IN MCNP4A	9
3.1 PARTICLE TRANSPORT IN MONTE CARLO CODES	9
3.2 PARTICLE CREATION MECHANISMS	9
3.3 PROGRAM FLOW OF PHOTONEUTRON PRODUCTION	9
3.4 INPUT CARDS FOR PHOTONEUTRON PRODUCTION	9
3.5 ACCOUNTING ARRAYS FOR PHOTONEUTRON STATISTICS	11
3.5.1 Problem Summary Array	11
3.5.2 Weight Balance in Each Cell	12
3.5.3 Neutrons Produced in Photon Collisions by Cell	12
3.5.4 Neutrons Produced in Photon Collisions by Energy	12
4. VERIFICATION AND VALIDATION OF THE PHOTONEUTRON OPTION	13
4.1 YIELD OF PHOTONEUTRON SOURCES	13
4.1.1 The Characterization of Photoneutron Sources	13
4.1.2 Description of the Calculations	14
4.1.3 Results of Photoneutron Yields	15
4.2 NEUTRON FLUXES IN THE ANS REACTOR REFLECTOR VESSEL	15
4.2.1 The Two-Element ANS Reactor Model	16
4.2.2 Description of the Calculations	17
4.2.3 Neutron Flux Results	18
5. CONCLUSION	23
6. REFERENCES	25
Appendix A. THE MCNP-UPDATE PATCH-FILE	A-1
Appendix B. MCNP PHOTONEUTRON CROSS SECTIONS	B-1

Appendix C. MCNP INPUT FOR THE PHOTONEUTRON SOURCE CALCULATIONS	C-1
---	-----

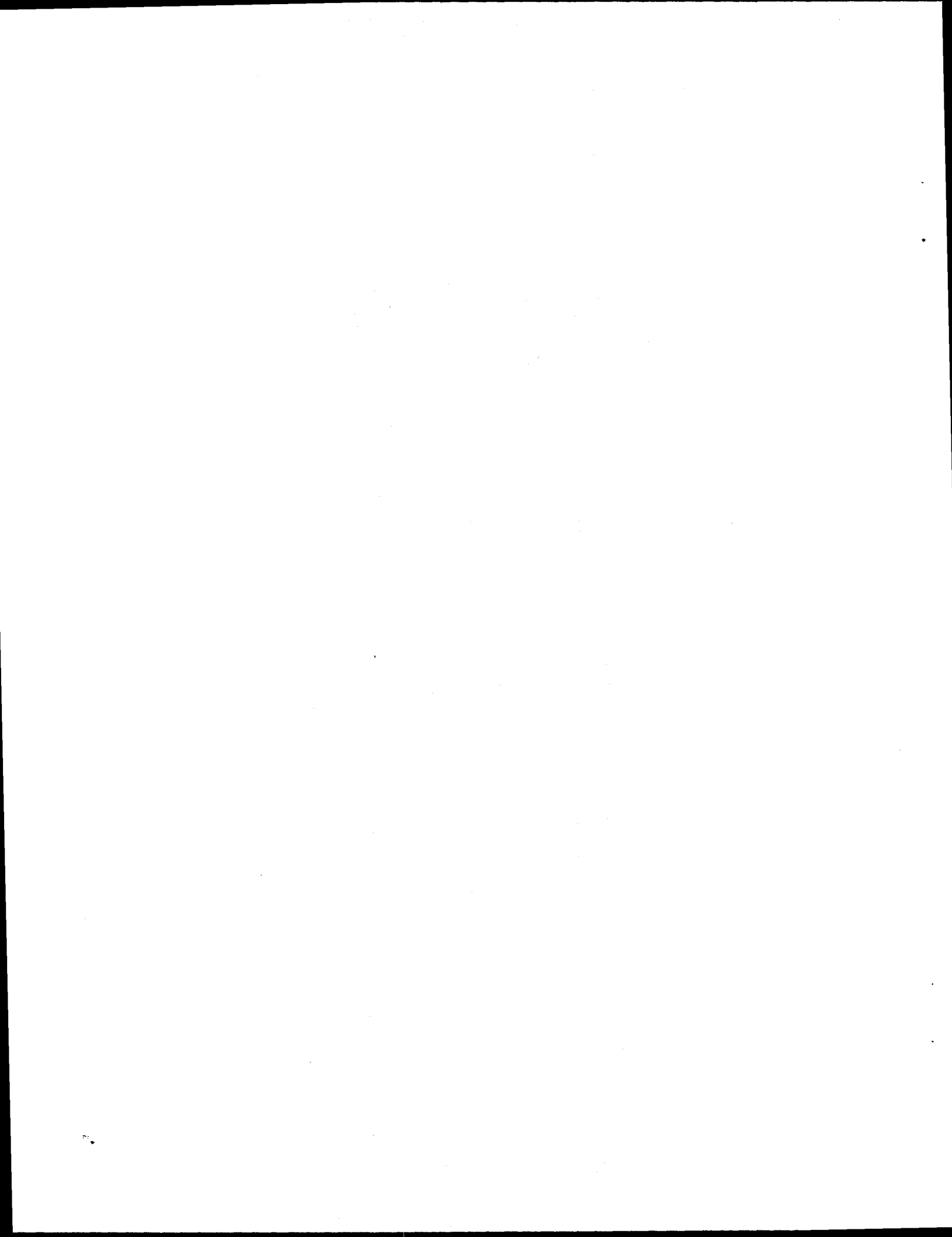
LIST OF TABLES

Table	Page
2.1 Nuclides with low photodisintegration threshold energies	3
4.1 Photon sources for photoneutron sources and their characteristic photon energies above 1.667 MeV	15
4.2 The effective Wattenberg constants measured by Bensch and Vesely ²³ and cal- culated with MCNP	16
4.3 Radii of the cylindrical flux tally zones in the reflector of the ANS reactor	18



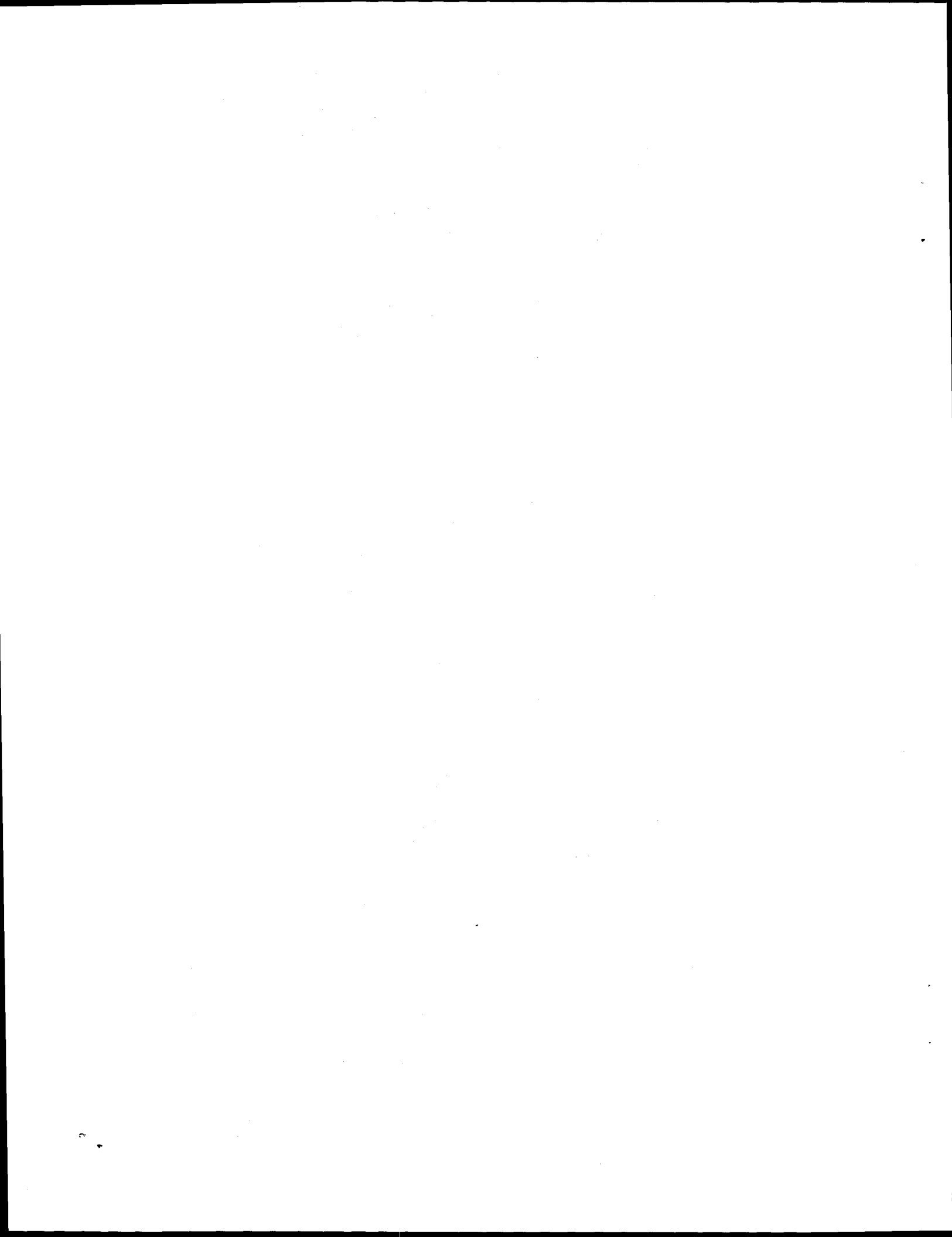
LIST OF FIGURES

Figure	Page
2.1 Photoneutron production cross section of deuterium derived analytically and compared with experimental data.	6
2.2 Ratio of the magnetically induced photoneutron cross section to the electrically induced photoneutron cross section $\sigma_{pn}^{M1}/\sigma_{pn}^{E1}$ for deuterium.	6
2.3 Photoneutron production cross section of beryllium evaluated from experimental data.	7
3.1 Program flow of the MCNP subroutine <i>colidp</i> with the photoneutron implementation.	10
4.1 MCNP model of the ANS reactor design with two fuel elements and without the experimental facilities in the reflector vessel.	17
4.2 Thermal neutron flux ($E < 0.625$ eV) in the heavy water reflector at the outer radial vessel wall calculated with MCNP and DORT including photoneutron production.	19
4.3 Fast neutron flux ($E = 0.1\text{--}0.9$ MeV) in the heavy water reflector	20
4.4 Epithermal neutron flux ($E = 0.625\text{--}550$ eV) in the heavy water reflector at the outer radial vessel wall calculated with MCNP and DORT including photoneutron production.	20
4.5 Fast neutron flux ($E = 0.550\text{--}17$ keV) in the heavy water reflector at the outer radial vessel wall calculated with MCNP and DORT including photoneutron production.	21
4.6 Fast neutron flux ($E = 17\text{--}100$ keV) in the heavy water reflector at the outer radial vessel wall calculated with MCNP and DORT including photoneutron production.	21
4.7 Fast neutron flux ($E = 0.1\text{--}0.9$ MeV) in the heavy water reflector at the outer radial vessel wall calculated with MCNP and DORT including photoneutron production.	22
4.8 Fast neutron flux ($E = 0.9\text{--}6.43$ MeV) in the heavy water reflector at the outer radial vessel wall calculated with MCNP and DORT including photoneutron production.	22



NOMENCLATURE

N	= element identifier
Z	= number of protons in nucleus
A	= number of protons and neutrons in nucleus
ν	= integer
e^-	= electron
e^+	= positron
n	= neutron
m_n	= neutron mass
E_{pn}	= energy of the photoneutron
γ	= photon
E_γ	= energy of photon
Q	= threshold energy of photoneutron production reaction
c	= velocity of light
θ	= angle between photon and photoneutron flight direction
$\sigma_{pn}(E_\gamma, \theta)$	= photoneutron cross section
$\sigma_{pn}^{max}(\theta)$	= maximal value of the photoneutron cross section regarding the angle θ
$\sigma_{pn}^{M1}(E_\gamma)$	= photoneutron cross section caused by a magnetic dipole transition
$\sigma_{pn}^{E1}(E_\gamma)$	= photoneutron cross section caused by a electric dipole transition
μ_p	= magnetic dipole moment of the proton
μ_n	= magnetic dipole moment of the neutron
μ_N	= nuclear magneton
ρ	= classical deuteron radius
1a	= singlet scattering length of deuterium
3r_o	= triplet effective range of the potential for deuterium
M	= reduced mass of the proton-neutron system
\hbar	= Planck's constant
K	= magnitude of isotropic photoneutron direction
L	= magnitude of anisotropic photoneutron direction
m	= mass
r	= distance
S	= activity
μ_w	= Wattenberg constant
μ_w^{eff}	= effective Wattenberg constant
ϵ	= ratio of activity above threshold energy and total activity
d	= density
N_d	= number density
Y	= photoneutron source strength
G_1	= reduction factor caused by self-shielding of photons in photoneutron sources
G_2	= reduction factor caused by self-shielding of photoneutrons in photoneutron sources



ABSTRACT

A photoneutron production option was implemented in the MCNP4A code, mainly to supply a tool for reactor shielding calculations in beryllium and heavy water environments of complicated three-dimensional geometries.

Photoneutron production cross sections for deuterium and beryllium were created. Subroutines were developed to calculate the probability of photoneutron production at photon collision sites and the energy and flight direction of the created photoneutrons. These subroutines were implemented into MCNP4A. Some small program changes were necessary for processing the input to read the photoneutron production cross sections and to install a photoneutron switch. Some arrays were installed or extended to sample photoneutron creation and loss information, and output routines were changed to give the appropriate summary tables.

To verify and validate the photoneutron production data and the MCNP4A implementations, the yields of photoneutron sources were calculated and compared with experiments. In the case of deuterium-based photoneutron sources, the calculations agreed well with the experiments; the beryllium-based photoneutron source calculations were up to 30% higher compared with the measurements. More accurate beryllium photoneutron cross sections would be desirable. To apply the developed method to a real shielding problem, the fast neutron fluxes in the heavy-water-filled reflector vessel of the Advanced Neutron Source reactor were investigated and compared with published DORT calculations. Considering the complete independence between the calculations, the merely 10 to 20% lower fluxes obtained with MCNP4A, compared against the DORT results, were more than satisfactory, as the discrepancy is based primarily on differences in the calculated thermal neutron fluxes.

1. INTRODUCTION

The disintegration of nuclei and the production of neutrons from photon-induced reactions are well known phenomena in physics leading to the development of monoenergetic neutron sources and having implications in reactor physics and in shielding. A nucleus absorbing a photon and releasing a neutron gives a direct insight into the binding energies of the highest level neutrons in the nucleus, which corresponds to the threshold energy of the reaction for the particular nucleus.

The nuclides deuterium and beryllium have particularly low threshold energies of 2.225 and 1.667 MeV, respectively, and are the materials for which the photoneutron production reaction was first discovered.^{1,2} This enabled researchers to build photoneutron sources based on a high-energy-gamma emitter and targets of heavy water or beryllium, which were widely used when there was a demand for monoenergetic neutrons. Because photon energies above the threshold are very likely provided either by the gammas released in the fission reaction or by neutron activation of various structural materials such as aluminum or steel and because heavy water and beryllium are two of the most effective moderator and reflector materials in nuclear reactors, photoneutron production can be important in certain reactor designs. Although the photoneutron production cross sections are merely in the range of 10^{-3} barn, photoneutrons can have a rather significant effect, especially in reactor shielding applications. The effect of photoneutrons on reactor dynamics in large heavy water and beryllium systems are usually not negligible³ but can be treated by forming a group of delayed neutrons with especially long delays because of the neutron's diffusion time.

For the design of the Advanced Neutron Source (ANS) reactor,⁴ which has a large inventory of heavy water, the effect of photoneutrons has to be included. In two-dimensional discrete-ordinates calculations of the unperturbed cylindrical reactor geometry, photoneutron production was included by modifying the coupled neutron/gamma multigroup cross section. Additional upscattering terms from the gamma groups into the neutron groups were introduced. For convergence of the flux solution, many iterations over all energy groups have to be performed, resulting in a procedure that is computationally very time consuming because of the many groups of upscattering.

Because of all the experimental facilities in the reflector vessel, the ANS reactor is a complicated three-dimensional geometry. For shielding calculations of this kind of geometry, the Monte Carlo code MCNP4A⁵ was modified to make it capable of dealing with photoneutron production, which is described in this report.

Section 2 summarizes the physics of photoneutron production as far as it is necessary for the understanding of the coding. Emphasis is placed on the description of the currently available photodisintegration cross sections for deuterium and beryllium, although the program treats cross section data for other isotopes as well. Section 3 deals with the implementation of the photoneutron option in MCNP, with a description of changed and new input cards and output arrays. Section 4 describes the verification and validation work of the photoneutron option. Section 4.1 compares calculated yields of photoneutron sources with experimental values; Sect. 4.2 shows results of flux calculations from MCNP4A for the ANS reactor to (1) demonstrate the new option in a reactor calculation and (2) compare the neutron fluxes in the heavy water vessel obtained in these calculations with DORT calculations. Section 5 presents the conclusion of the work.

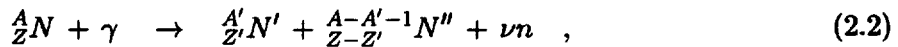


2. THE PHOTODISINTEGRATION REACTION

In general, the photodisintegration reaction of a nuclide N with atomic number A and charge number Z is the inverse of a neutron absorption reaction:⁶



Instead of creating a nucleus with one additional neutron and releasing its excess binding energy into a photon, as for neutron absorption, in the photodisintegration reaction a high-energy photon is absorbed and a neutron is released with a kinetic energy that is the difference between the photon energy and the neutron's binding energy in the nucleus. However, other reaction paths releasing a neutron in a photon-induced reaction are also possible, such as the photofission reaction:⁷



or (n,2n) reactions. For most nuclides the binding energy of the highest level neutron, which plays the role of a threshold energy for the photodisintegration reaction, is about 7 MeV⁸ and therefore of minor interest in reactor physics. But nature provides some materials that have much lower threshold energies (see Table 2.1).

Table 2.1. Nuclides with low photodisintegration threshold energies

Nuclide	Threshold (MeV)
2D	2.225
6Li	5.7
9Be	1.667
^{13}C	4.9

From impulse and energy conservation, the following approximate formula for the photoneutron energy can be derived:⁹

$$E_{pn} \approx \frac{A-1}{A} \left(E_\gamma - Q - \frac{E_\gamma^2}{2m_n c^2 (A-1)} + \frac{E_\gamma}{A} \sqrt{\frac{2(A-1)}{(m_n c^2 A)(E_\gamma - Q)}} \cos\theta \right) , \quad (2.3)$$

where

- A = mass of the target nucleus,
- E_γ = energy of the photon,
- E_{pn} = energy of the neutron,
- Q = threshold energy,
- m_n = neutron mass,
- c = velocity of light,
- θ = angle between photon and neutron flight direction.

The probability of an excitation of a nucleus from bound states into the continuum by magnetic dipole (M1) and electric dipole (E1) transitions is far more probable than higher-order transi-

tions.¹⁰ Therefore, the distribution of the neutron's outgoing direction can be described by the general angular dependence⁶

$$\frac{d\sigma_{pn}(\theta)}{d\Omega} = L + K \sin^2(\theta) , \quad (2.4)$$

where the magnetic dipole (M1) transition has an isotropic character described by the constant K and the electric dipole transition has a typical dipole (E1) character described by L , with θ being the angle between the incoming photon direction and the outgoing neutron direction. The angular distribution can be rewritten in the form

$$\frac{d\sigma_{pn}(\theta)}{d\sigma_{pn}^{max}(\theta)} = 1 - \frac{K}{K + L} \cos^2(\theta) , \quad (2.5)$$

where $\sigma_{pn}^{max}(\theta)$ is the maximal photoneutron cross section regarding the angle θ . Equation (2.5) can easily be applied in the Monte Carlo game to select the neutron's direction $\cos(\theta)$ by the rejection method.¹¹

To characterize the photodisintegration reaction of any material, two sets of energy dependent data are sufficient: the photoneutron production cross sections and the ratio $K/(K + L)$. Although the modified MCNP program allows for photoneutron production cross section data as input the cross section data for the nuclides 2D and 9Be used for verification calculations are described.

2.1 PHOTONEUTRON PRODUCTION CROSS SECTION OF DEUTERIUM

The deuterium nucleus, consisting of only a proton and a neutron, is a widely studied system in the field of atomic physics.^{10,12} The level of understanding culminated in a few theoretical models and analytical formula that fit rather well with experimental data. Assuming that neutrons and protons are arranged as fermions with spin of 1/2 in potential discrete energy levels, the ground state of the deuterium is known to be a bound triplet 3S state from which a transition into the continuum can take place into the 0S state. This transition involves only a spinflip with change in the spin state of one and is therefore called magnetic dipole (M1) transition. Its cross section is calculated as¹⁰

$$\sigma_{pn}^{M1}(E_\gamma) = \frac{2}{3} \frac{\pi}{137} (\mu_p - \mu_n)^2 \left(\frac{\hbar}{2Mc} \right)^2 \frac{\sqrt{Q(E_\gamma - Q)}}{E_\gamma} \frac{Q(1 - \frac{1}{a} \frac{a}{\rho})^2}{Q + (\frac{1}{a} \frac{a}{\rho})^2 (E_\gamma - Q)} , \quad (2.6)$$

with

Q	$= 2.225$ MeV	threshold energy of deuterium,
μ_p	$= 2.7927 \mu_N$	magnetic dipole moment of the proton,
μ_n	$= -1.9131 \mu_N$	magnetic dipole moment of the neutron,
μ_N	$= 5.0508 \text{ A m}^2$	nuclear magneton,
1a	$= -23.69 \text{ } 10^{-15} \text{ m}$	singlet scattering length,
ρ	$= 4.31 \text{ } 10^{-15} \text{ m}$	deuteron radius,
M	$= m_n/2$	reduced mass of the proton-neutron system,
m_n	$= 1.67 \text{ } 10^{-27} \text{ kg}$	neutron mass,
\hbar	$= 1.054 \text{ } 10^{-34} \text{ Js}$	Planck's constant.

Higher photon energies enable the transitions from the 3S -groundstate to the 3P -continuum state, which is called an electric dipole (E1) transition resulting from a change of the orbital angular momentum of one. The cross section can be derived as¹⁰

$$\sigma_{pn}^{E1}(E_\gamma) = \frac{8\pi}{3} \frac{1}{137} \rho^2 \left(\frac{\sqrt{Q(E_\gamma - Q)}}{E_\gamma} \right)^3 \frac{1}{1 - 3r_o/\rho} , \quad (2.7)$$

with

$$\begin{aligned} \rho &= \hbar/\sqrt{2MQ} && \text{is the deuteron radius,} \\ {}^3r_o &= 1.70 \cdot 10^{-13} \text{ cm} && \text{is the triplet effective range.} \end{aligned}$$

The cross sections for the magnetic and electric dipole transition add up to the total photodisintegration cross section:

$$\sigma_{pn}(E_\gamma) = \sigma_{pn}^{M1}(E_\gamma) + \sigma_{pn}^{E1}(E_\gamma) . \quad (2.8)$$

Because the magnetic dipole transition gives an isotropic distribution of the neutron's flight direction and because the electric dipole transition causes a dipole characteristic of the neutron's angular flight direction, the differential cross section can be written as¹⁰

$$\frac{d\sigma_{pn}(\theta)}{d\Omega} = \frac{1}{4\pi} \sigma_{pn}^{M1} + \frac{3}{8\pi} \sigma_{pn}^{E1} \sin^2\theta . \quad (2.9)$$

Figures 2.1 and 2.2 compare the analytically derived σ_{pn} and of $\sigma_{pn}^{M1}/\sigma_{pn}^{E1}$ with some measured values.

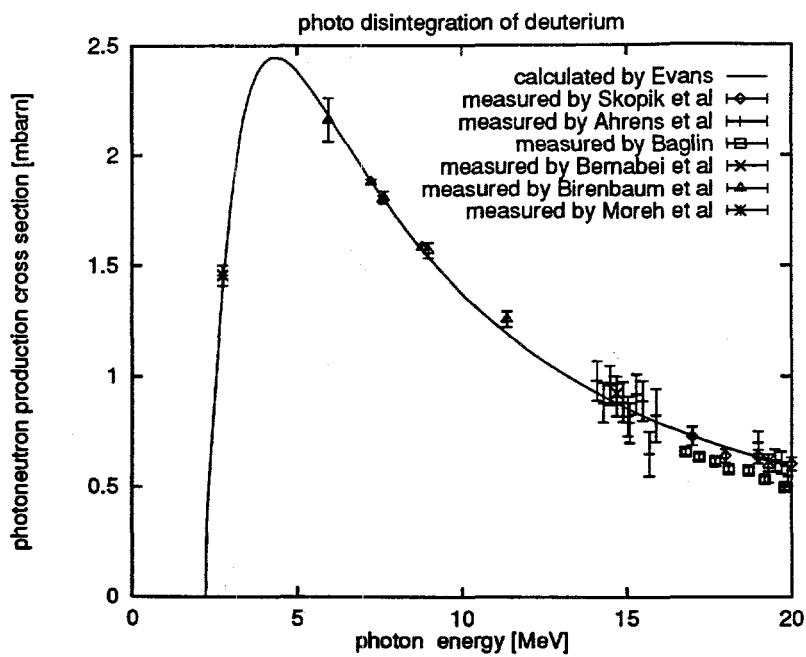


Fig. 2.1. Photoneutron production cross section of deuterium derived analytically and compared with experimental data.

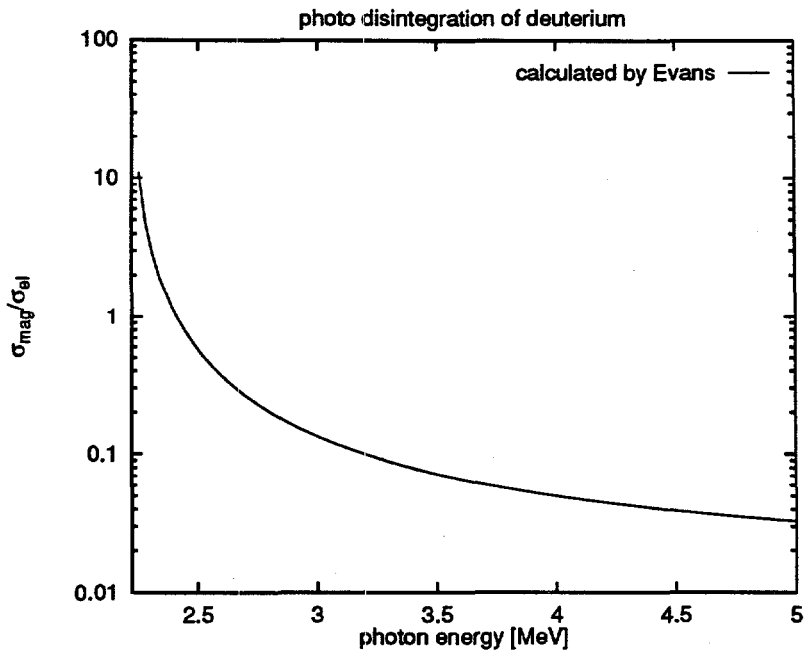


Fig. 2.2. Ratio of the magnetically induced photoneutron cross section to the electrically induced photoneutron cross section $\sigma_{pn}^{M1}/\sigma_{pn}^{E1}$ for deuterium.

2.2 PHOTONEUTRON PRODUCTION CROSS SECTION OF BERYLLIUM

Because beryllium is an isotope consisting of nine protons and neutrons, a simple analytical approach, as used for deuterium, cannot be found.¹³ Calculations with theoretical models do not agree well enough with experimental cross sections, so measured evaluated data for the cross section of beryllium must be used. The cross sections used in this work are taken from the Lawrence Livermore National Laboratory (LLNL) Physical Data Note PD-173,¹⁴ which gives the following note about their evaluation: "In choosing data for the evaluation, priority was given to the monoenergetic photon source results of Edge,[¹⁵] Gibbons,[¹⁶] John,[¹⁷] Bösch,[¹⁸] Berman [¹⁹] and Fujishiro.[²⁰] From 1.66 to 2 MeV an eyeball average was taken of the data from Gibbons, John, Berman and Fujishiro. For the 4 to 9 MeV interval the points were taken directly from Bösch and partly from Edge. In the 2 to 4 MeV interval an eyeball average was taken of unfolded bremsstrahlung results of Jakobson [²¹] and Hughes [¹³], while for 10 to 16 MeV an average was estimated from those of Costa [²²] and Hughes, relying principally on the detailed comparison graphics in Hughes' figure 5."

In this work, the energy range was extended to 20 MeV using data from Hughes. The composite result is plotted in Fig. 2.3. In Jakobson, some information about the angular dependence of the neutron's direction of the peaks of the cross section below 5 MeV is given. The directions of neutrons with energies of 1.70 and 4.0 MeV are isotropically distributed with $K/(K + L)=0.0$, whereas those of the 2.95 MeV peak are a mixture of isotropic and dipole, characteristic of the ratio $K/(K + L)=0.5$. As no further information was available, an isotropic direction distribution is assumed for energies above 3.5 MeV.

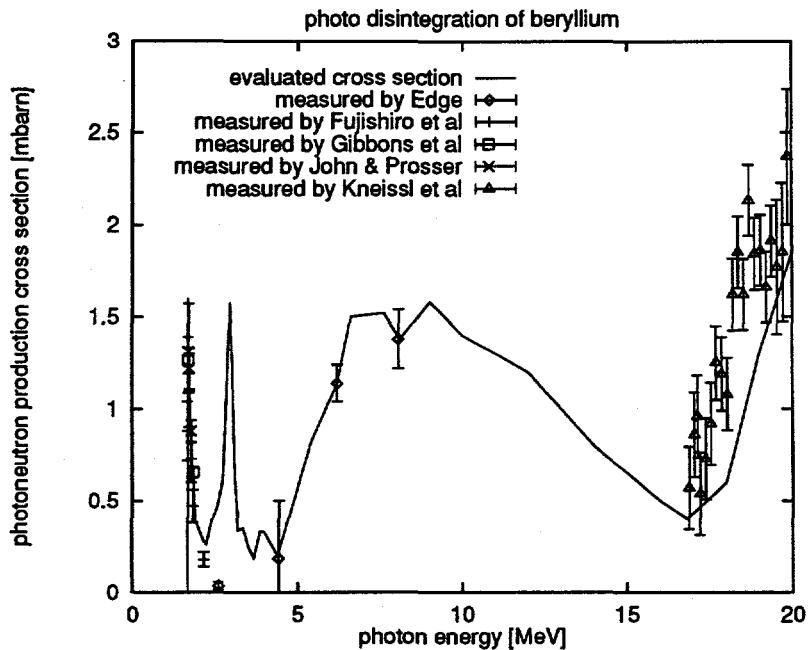


Fig. 2.3. Photoneutron production cross section of beryllium evaluated from experimental data.



3. IMPLEMENTATION IN MCNP4A

3.1 PARTICLE TRANSPORT IN MONTE CARLO CODES

In MCNP4A⁵ a particle is described by the weight *wgt*; the energy *erg*; its location *x, y, z*; its flight direction *u, v, w*; the lifetime *t*; and in coupled problems, the particle identifier *par*. A particle is started in a source subroutine (e.g., a fission source or a fixed source) and is transported to its next collision site considering the mean free path in the particle's flight direction. At the collision sites, several events are accounted for: weight loss from absorption reactions, secondary particle creation, and energy and direction change caused by scattering. The particles' histories are terminated by escape from the system, by energy/weight/time cutoff or by Russian roulette mechanisms using variance reduction methods. The main goal is to sample particle information with the help of estimators in regions of interest.

3.2 PARTICLE CREATION MECHANISMS

In modelling the physics processes, there are several ways in MCNP4A to create a particle in interactions with materials:

(n, f)	= fission reaction,
(n, xn)	= neutron multiplication,
(n, γ)	= neutron capture with photon production,
$(\gamma, 2\gamma')$	= second fluorescence,
(γ, e^-)	= first fluorescence,
$(e^+ e^-, 2\gamma)$	= $e^+ e^-$ annihilation,
free e^-	= bremsstrahlung,
bound e^-	= atomic transitions,
...	= some electron producing effects.

To make the list of production mechanisms more complete, the photoneutron production (γ, n) creation path was implemented into MCNP4A.

3.3 PROGRAM FLOW OF PHOTONEUTRON PRODUCTION

The kernel of photoneutron production has been implemented in MCNP4A in subroutine *colidp*, which processes the photon collisions. Figure 3.1 shows the program flow. Photoneutron production is executed basically in two subroutines: *getpnx*, which looks for the photoneutron data of the present collision nuclide, and *nmaker*, which performs the photoneutron production, saving a neutron if photoneutron production was successful.

3.4 INPUT CARDS FOR PHOTONEUTRON PRODUCTION

Some additional input has to be provided to apply the photoneutron production option. To allow switching photoneutron production on and off and to tell MCNP4A which way to apply the photoneutron option, the *phys:p*-card was extended by the forth entry of *ineut*:

phys:p emcpf ides nocoh ineut

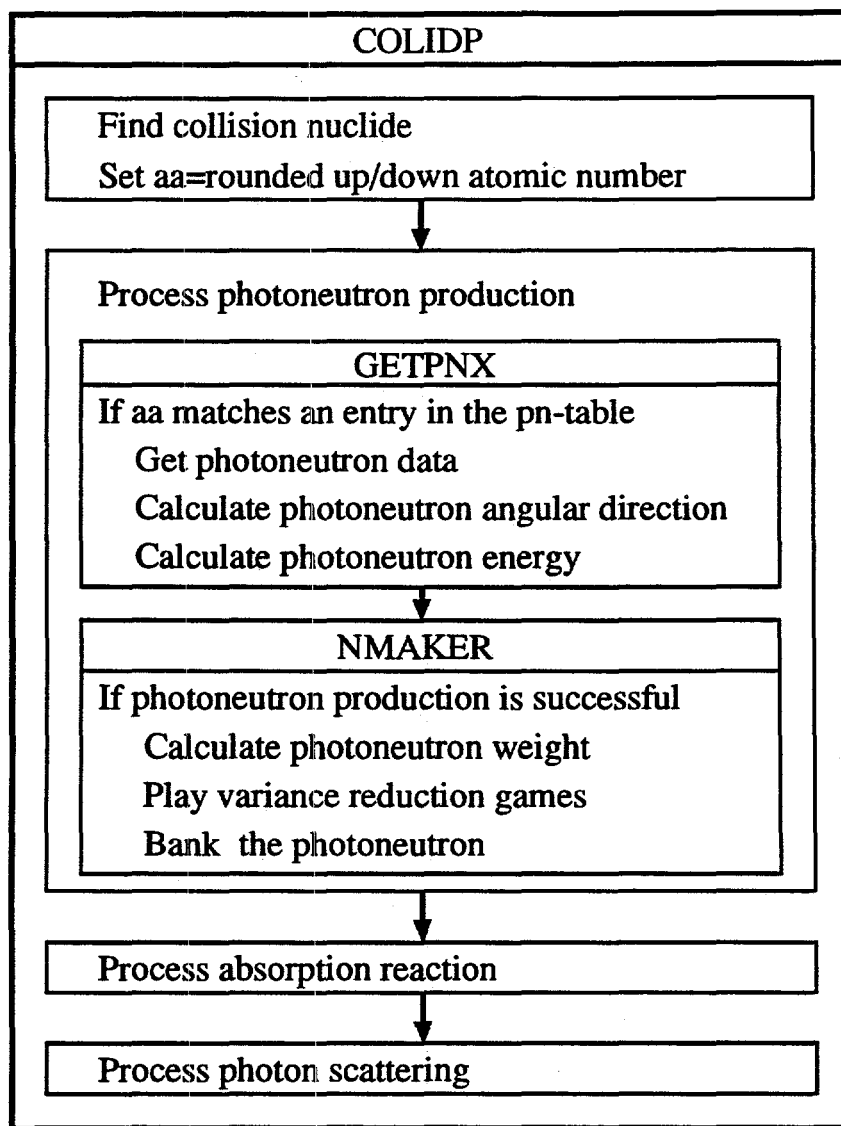


Fig. 3.1. Program flow of the MCNP subroutine *colidp* with the photoneutron implementation.

The entry *ineut* envoys the following actions connected to the given value:

- 0 no photoneutron production
- 1 photoneutron production with isotropic angular distribution
- +1 photoneutron production with anisotropic angular distribution.

To make the photoneutron option more flexible, the photoneutron cross sections have to be user-supplied data in MCNP cross section format that are read in and prepared together with the conventional cross section processing. The *pn*-card was newly introduced to provide the photoneutron cross section identifiers for those isotopes, which MCNP4A has to treat as photoneutron producing isotopes. The *pn*-card is used in the following form:

pn *pnid1.zzn* *pnid2.zzn* ... *pnidk.zzn*

pnidk is any six-letter string
zz is a two-figure number, and
n is index for pn-cross section.

For every identifier there has to be an entry in the cross section directory *xsdir*, where MCNP4A looks for the information identifying the cross sections file. Information about the structure of the MCNP photoneutron cross section files is given in Appendix B. MCNP4A automatically sets up the photoneutron cross sections for the number of entries given. Note that MCNP4A identifies the photoneutron-producing nuclides by the atomic number of the collision nuclide. The program rounds the atomic number of the current collision nuclide to the nearest integer and picks the photoneutron cross section of the first entry that matches the entries in the table of photoneutron cross sections. Because conflicts may arise when some nuclides in the problem set up have the same atomic number, the user is warned during the cross section processing if such conflicts occur.

3.5 ACCOUNTING ARRAYS FOR PHOTONEUTRON STATISTICS

To set up statistics of the particle transport and to give an overview of the program performance, MCNP4A provides the user with abundant tabulated information. To be able to examine the performance of the photoneutron production option, some of the accounting arrays had to be extended, and subroutines that evaluate and print the arrays had to be modified or written. The following paragraphs describe the changes of the arrays and type of information stored in the new locations. The output is self-explanatory.

3.5.1 Problem Summary Array

The photoneutron production is a new creation mechanism sampled in the array *pax(i,15,1)*
i=1..3:

- i=1* stores the number of tracks created,
- i=2* stores the weight created, and
- i=3* stores the energy created.

3.5.2 Weight Balance in Each Cell

In the array $pwb(1,18,icl)$, the weights of created photoneutrons are stored for each cell icl .

3.5.3 Neutrons Produced in Photon Collisions by Cell

The array $pcc(j,mxa)$, which holds the information of photons produced in neutron collisions in each cell, is extended from $j=3$ to $j=6$ (mxa =number of cells in the problem) to store

$j=4$, number of neutrons produced in photon collisions
 $j=5$, weight of neutrons produced in photon collisions, and
 $j=6$, weight * energy of neutrons produced in photon collisions.

3.5.4 Neutrons Produced in Photon Collisions by Energy

The array $febl(j,16)$ is extended from $j=2$ to $j=4$. The $febl$ array samples the photoneutron production data resolved in energy bins such that

$j=3$ stores the number of photon-induced neutrons in each energy bin, and
 $j=4$ stores the weight of photon-induced neutrons in each energy bin.

The energy-bin bounds for the photoneutron production data are:

bin	energy (MeV)	bin	energy (MeV)
1	20.00	9	1.50
2	15.00	10	1.00
3	10.00	11	0.60
4	7.00	12	0.30
5	5.00	13	0.10
6	4.00	14	0.05
7	3.00	15	0.01
8	2.00	16	0.00

4. VERIFICATION AND VALIDATION OF THE PHOTONEUTRON OPTION

To verify the program implementation and the photoneutron production cross sections generated, Sect. 4.1 describes calculations of the yield of photoneutron sources and compares results with experimental data. Furthermore, Sect. 4.2 gives an example of how to apply the photoneutron option of MCNP4A in reactor shielding calculations. The neutron fluxes in the D₂O-filled reflector vessel of the ANS reactor were calculated and compared with the neutron fluxes obtained in a DORT calculation.

4.1 YIELD OF PHOTONEUTRON SOURCES

Photoneutron sources in benchmark experiments consist of a highly active gamma source, originating from decaying radionuclides, surrounded by a target material such as beryllium or heavy water. This type of source has a size of only a few centimeters so that photons and the produced photoneutrons leave the system before being multiply scattered and/or absorbed. If the source produces only gammas of one discrete energy above the threshold energy of the target material, the generated photoneutrons are monoenergetic, which makes this type of neutron source very valuable for certain applications.

Because the physical size of the photoneutron source is small and scattering events are rare, photoneutron sources are suitable for verifying the implementation of the photoneutron production option of MCNP4A and for testing the photoneutron production pointwise cross sections. The problem is small in terms of input requirements and run time.

4.1.1 The Characterization of Photoneutron Sources

The effectiveness of a photoneutron source is the ratio of photoneutrons produced per activity of the gamma source. A quantity of this kind depends on the choice of source and target materials and on the geometry.

To separate the material dependence from the geometry dependence, the neutron source strength is defined²³ as

$$Y = \frac{\mu_w S m}{r^2} , \quad (4.1)$$

with

- Y = photoneutron source strength,
- μ_w = so-called Wattenberg constant,
- S = gamma source activity,
- m = mass of target material,
- r = distance from gamma source to target.

The Wattenberg constant μ_w gives the yield of neutrons of a specific gamma point source of 1 Ci of activity placed at a distance of 1 cm from 1 gram of a thin target material.^{24,25} Given the photoneutron cross section, μ_w can be calculated as

$$\mu_w = \frac{3.7E10 \epsilon N_d \sigma_{pn}}{4\pi d} , \quad (4.2)$$

with

- ϵ = ratio of activity above threshold energy and total activity,
- N_d = number density of target material,
- d = density of target material,
- σ_{pn} = photoneutron production cross section.

Because a real photoneutron source consists of a volume-distributed gamma source and a finite thick layer of target material, the Wattenberg constant has to be corrected. The spherically distributed gamma source, with radius r_1 and surrounded by a layer of target material with radius r_2 , can be reduced to a point gamma source in the center of a sphere of radius r_1^{eff} surrounded by target material of radius r_2^{eff} , where the radius r_1^{eff} is defined as the mean geometrical photon path in the source material

$$r_1^{eff} = \frac{3}{4} r_1 \quad , \quad (4.3)$$

and the length $r_2^{eff} - r_1^{eff}$ is the mean geometrical photon path through the target material, where

$$r_2^{eff} = \frac{r_2}{2} + \frac{3}{4} \frac{r_2^4}{r_1^3} C \quad , \quad (4.4)$$

where

$$C = \frac{1}{4} (1 - b^2)^2 \ln \left(\frac{1-b}{1+b} \right) + \frac{3b - b^3}{6} \quad , \quad (4.5)$$

and

$$b = \frac{r_1}{r_2} \quad . \quad (4.6)$$

The real photoneutron source experiences a decrease of the yield because of photon reactions in the photon source described by the reduction factor G_1 and caused by the self-shielding effects in the target material by the reduction factor G_2 .²³ The derivation of both reduction factors is given in Bensch and Vesely.²³ The effective Wattenberg constant is defined as

$$\mu_w^{eff} = \mu_w G_1 G_2 \quad . \quad (4.7)$$

Combining the previous definitions, the photoneutron source strength of a real arrangement can be written as

$$Y = 4\pi d \mu_w^{eff} S \epsilon (r_2^{eff} - r_1^{eff}) \quad . \quad (4.8)$$

4.1.2 Description of the Calculations

The photon sources given in Table 4.1 and their characteristic photon energies have been used for the benchmark experiments²³ and the MCNP4A calculations.

The source material was enclosed in a spherical tin container of 10 mm inner diam and a wall thickness of 1 mm and surrounded by a 20-mm-thick shell of target material. For this geometry,

Table 4.1. Photon sources for photoneutron sources and their characteristic photon energies above 1.667 MeV

Source	Efficiency	Photon energies (MeV)	Probability
^{124}Sb	0.5473	1.6910	0.4903
		2.0910	0.0573
^{72}Ga	0.5267	1.8611	0.0523
		2.1095	0.0103
		2.2017	0.2611
		2.4910	0.0748
		2.5078	0.1282
^{140}La	0.0345	2.5217	0.0345
^{116}In	0.1777	1.7524	0.0239
		2.1123	0.1538
^{56}Mn	0.4365	1.8107	0.2719
		2.1131	0.1434
		2.5229	0.0099
		2.6575	0.0065
		2.9598	0.0031
		3.3696	0.0017
^{24}Na	0.9986	2.7541	0.9986

the effective radii have the values: $r_1^{eff} = 3.75$ mm and $r_2^{eff} = 24.85$ mm. The input description for this MCNP run is in Appendix C.

4.1.3 Results of Photoneutron Yields

The experimental and calculational results of the investigated photoneutron sources are summarized in Table 4.2. The statistical uncertainty of one standard deviation in the Monte Carlo calculations is of the order 1 to 2%.

The results show good agreement between experiment and calculation for the photoneutron sources with heavy water as target materials, whereas the calculations for the photoneutron sources with the beryllium targets are as much as 30% higher compared with the experiments. However, considering the energy dependence of the beryllium photoneutron cross sections with its sharp peaks in the energy range of 1.5 to 3 MeV, the results obtained are quite satisfying (see Fig. 2.3). More accurate beryllium photoneutron cross sections would be desirable.

4.2 NEUTRON FLUXES IN THE ANS REACTOR REFLECTOR VESSEL

The ANS reactor consists of two heavy water-cooled fuel elements (the two-element design was later replaced by a three-element design), which are placed in the center of a cylindrical heavy

Table 4.2. The effective Wattenberg constants measured by Bensch and Vesely²³ and calculated with MCNP

Photoneutron source	Density of source (mg/mm ³)	$\mu_w^{eff.} \cdot 10^{-5}$ [$\frac{mm^2}{s Ci mg}$]	
		experiment	calculation
²⁴ NaF - D ₂ O	2.56	22.09	22.61
¹²⁴ Sb - Be	6.69	10.32	10.32
²⁴ NaF - Be	2.56	10.13	13.87
⁷² Ga - D ₂ O	5.91	3.07	2.85
¹¹⁴ In - Be	7.28	0.825	1.26
¹⁴⁰ La ₂ O ₃ - Be	6.51	0.181	0.291

water reflector. In the large heavy water volume, photons from the fission reactions, neutron absorption reactions, and decay reactions produce photoneutrons. For distances far from the fuel element, fast neutron fluxes originating from the fission reaction have dropped to insignificant values because of moderation in the heavy water. However, the high-energy photons produced in neutron absorption reactions in the aluminum reflector vessel, which dominate the high-energy photon flux far from the core, enable photoneutrons to be produced in the photodisintegration of deuterium. As found in DORT calculations of a cylindrical model of the ANS reactor,²⁶ the photoneutrons build up a fast neutron flux, which can be orders of magnitude larger than the fast neutron fluxes originating from the fission reaction.

To demonstrate the developed method in a shielding problem, the fluxes in the ANS reactor⁴ near the outer radial reflector vessel wall were calculated with MCNP and compared with the fluxes obtained in the DORT calculations.²⁶

4.2.1 The Two-Element ANS Reactor Model

An MCNP model of the two-element ANS design was set up to match the DORT model.²⁶ The two cylindrical fuel elements were placed in the middle of a central core pressure boundary tube and surrounded by a heavy water reflector of 4.25 m height and 3.50 m diam, as shown in Fig. 4.1. In the model, the aluminum reflector vessel was assumed to be 25 mm thick and enclosed by 0.20 m of light water.

All core details were taken directly from the ANS model used in MCNP heating calculations.²⁷ The reflector volume was modeled as a full cylinder to match the DORT model. No experimental facilities or beam tubes in the reflector vessel were included. To use weight windows for the variance reduction methods, Russian roulette, and splitting and to define the zones of interest for tallying the fluxes, the heavy water reflector volume and the light water volume were subdivided.

The fluxes were tallied with the tracklength estimator in 12 cylindrical shells of 1.76 m height centered around the core midplane and with the radii given in Table 4.3 that match the mesh widths of the DORT model.

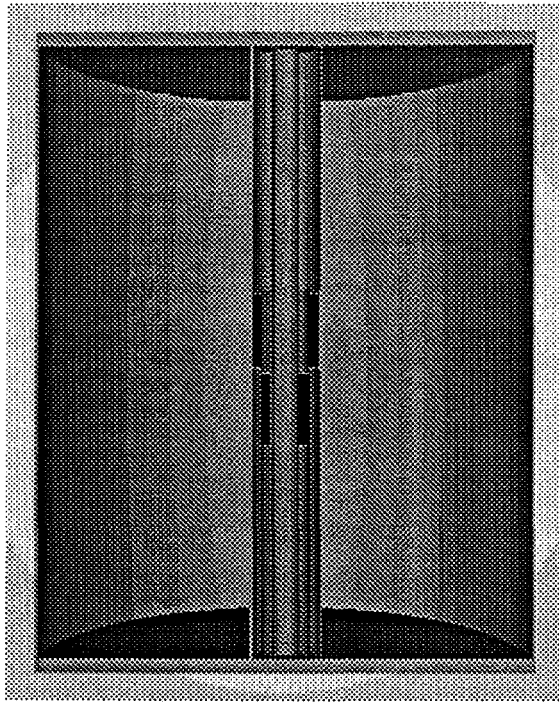


Fig. 4.1. MCNP model of the ANS reactor design with two fuel elements and without the experimental facilities in the reflector vessel.

4.2.2 Description of the Calculations

The calculation was performed with a fixed source, the source distribution of which was prepared by a previous DORT calculation. A set of photoneutron cross sections for deuterium was created for this calculation based on data published in Keepin²⁸ since the same data were used in the DORT calculations. These data are listed in Appendix B. These photoneutron cross sections are only slightly different from the analytically derived photoneutron cross sections described in Sect. 2.1.

To increase the number of histories in the tally cells, importances were increased about a factor of 3 from reflector cell to reflector cell in the direction towards the reflector vessel wall and weight windows were set up with the help of these importances. Bear in mind that the weight assigned to the photoneutrons at their production sites is farely small because of the small photoneutron cross section (with the weight of the photoneutrons being about a factor of 1000 lower than the weight of the photons). Thus, the neutron weight boundaries for Russian roulette have to be adjusted; otherwise, almost all photoneutrons would be killed immediately after their appearance.

Because the DORT calculation included the prompt fission photons as well as the delayed photons from the fission fragments and because the MCNP calculation takes into account only

Table 4.3. Radii of the cylindrical flux tally zones in the reflector of the ANS reactor

Tally no.	Inner and outer radii (mm)
1	1560 – 1580
2	1580 – 1600
3	1600 – 1620
4	1620 – 1640
5	1640 – 1660
6	1660 – 1680
7	1680 – 1700
8	1700 – 1710
9	1710 – 1720
10	1720 – 1730
11	1730 – 1740
12	1740 – 1750

the prompt fission gammas, a second MCNP calculation was performed with a delayed fission product photon source. The neutron fluxes obtained in this calculation were a factor of 1000 lower than the neutron fluxes in the first calculation and were therefore insignificant.

4.2.3 Neutron Flux Results

The neutron fluxes in the fast and epithermal energy range near the reflector vessel wall have a statistical error (statistical uncertainty of one standard deviation) of about 10%. In the center of the reflector vessel the statistical errors are larger; however, the thermal fluxes are more accurate, with a statistical error of about 2%.

The neutron fluxes in various energy groups are plotted vs the reactor radius for the DORT calculation without photoneutron production, for the DORT calculation with the photoneutron calculation, and for the MCNP calculation with photoneutron production. The MCNP calculation without photoneutron production results in fast and epithermal neutron fluxes of zero and is therefore not considered.

The thermal neutron fluxes obtained in the MCNP calculation were about 12% lower compared with the DORT fluxes, as shown in Fig. 4.2. This discrepancy also appeared in former comparisons²⁶ and could not be resolved. In Fig. 4.3, a comparison of the fast fluxes ranging in energy from 0.1 to 0.9 MeV shows differences between the flux calculations with photoneutrons and without photoneutrons of up to three orders of magnitude. Figure 4.3 does not include a curve of neutron fluxes in the case without photoneutrons calculated with MCNP because the fast neutron fluxes without photoneutrons were too low to be calculated with MCNP.

Because the photon flux with an energy above 2.225 MeV builds up primarily because of thermal neutron absorption, the difference in the thermal neutron fluxes between DORT and MCNP is directly reflected in the photoneutron production level and in the fast neutron fluxes, as can be seen in Figs. 4.4 – 4.8. Regarding the discrepancy in the thermal neutron flux

and its effect on the fast neutron flux, the MCNP calculations compare well with the DORT calculations.

Both MCNP calculations, the calculation with photoneutron production and the calculation without photoneutron production, consumed almost the same central processing unit time. Compared to the total number of scatterings, the number of photoneutrons produced is insignificant.

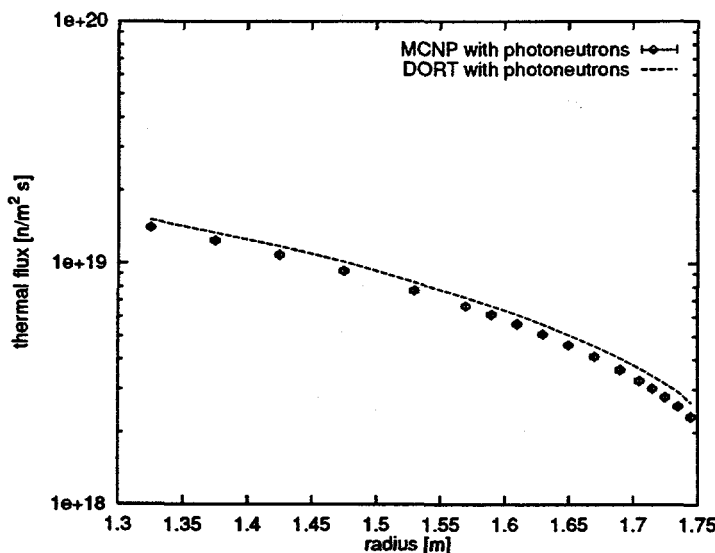


Fig. 4.2. Thermal neutron flux ($E < 0.625$ eV) in the heavy water reflector at the outer radial vessel wall calculated with MCNP and DORT including photoneutron production.

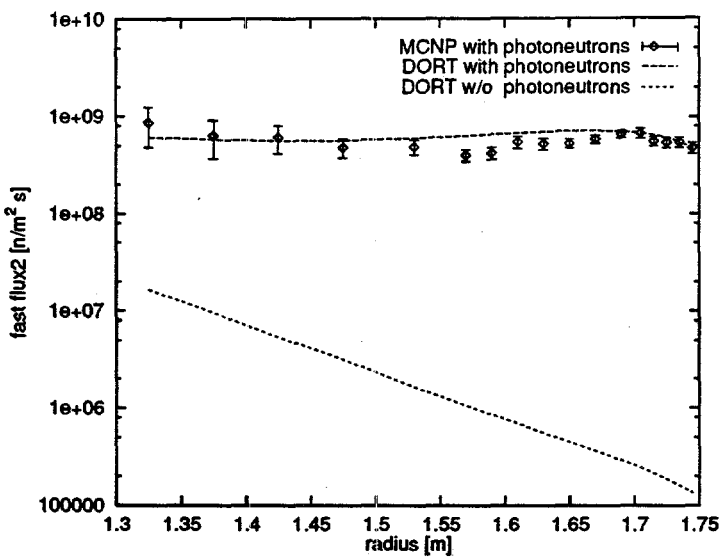


Fig. 4.3. Fast neutron flux ($E = 0.1\text{--}0.9$ MeV) in the heavy water reflector. Fluxes calculated with MCNP and DORT including photoneutron production are shown and compared to a DORT calculation without photoneutrons.

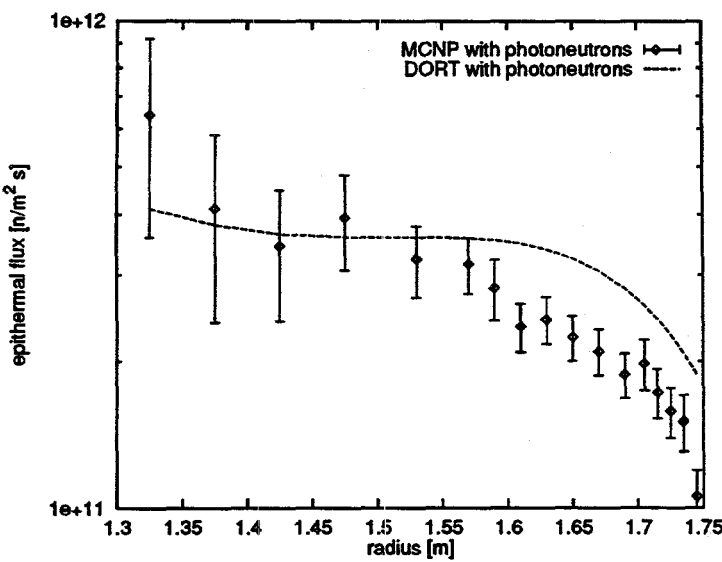


Fig. 4.4. Epithermal neutron flux ($E = 0.625\text{--}550$ eV) in the heavy water reflector at the outer radial vessel wall calculated with MCNP and DORT including photoneutron production.

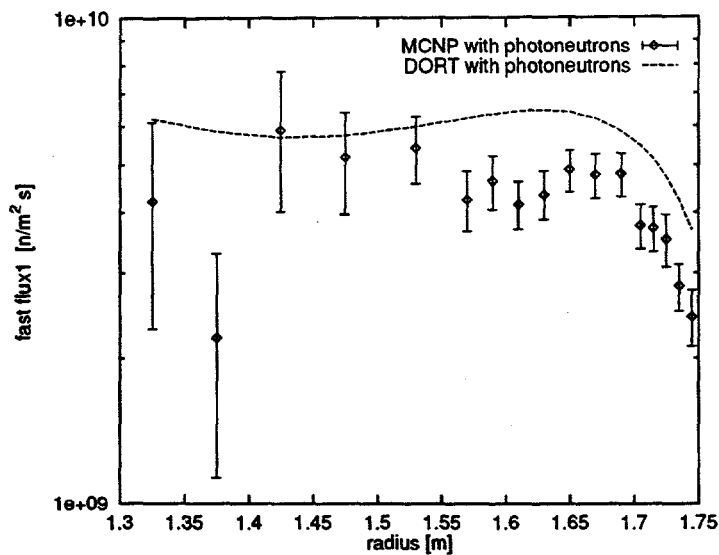


Fig. 4.5. Fast neutron flux ($E = 0.550\text{--}17\text{ keV}$) in the heavy water reflector at the outer radial vessel wall calculated with MCNP and DORT including photoneutron production.

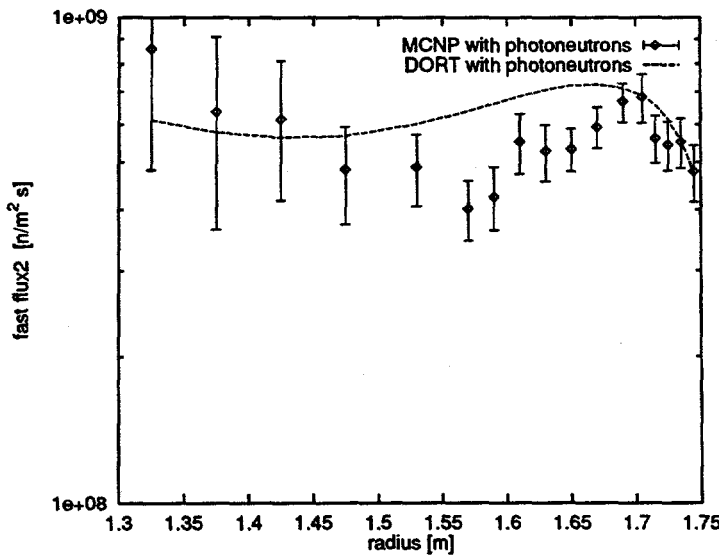


Fig. 4.6. Fast neutron flux ($E = 17\text{--}100\text{ keV}$) in the heavy water reflector at the outer radial vessel wall calculated with MCNP and DORT including photoneutron production.

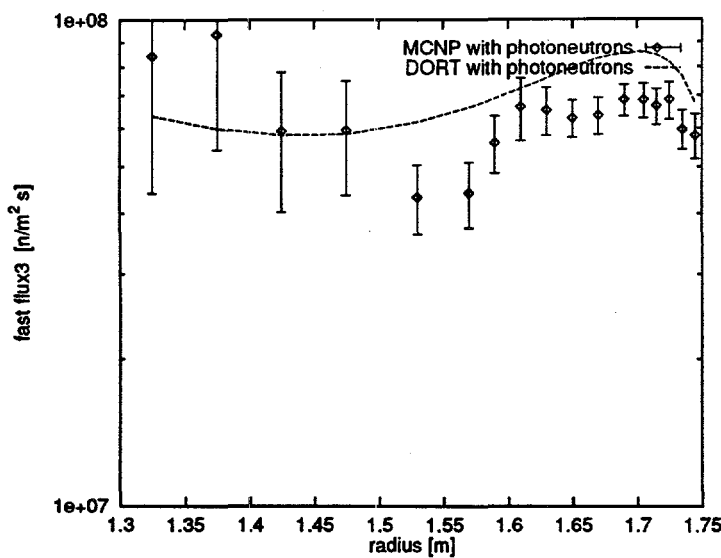


Fig. 4.7. Fast neutron flux ($E = 0.1\text{--}0.9$ MeV) in the heavy water reflector at the outer radial vessel wall calculated with MCNP and DORT including photoneutron production.

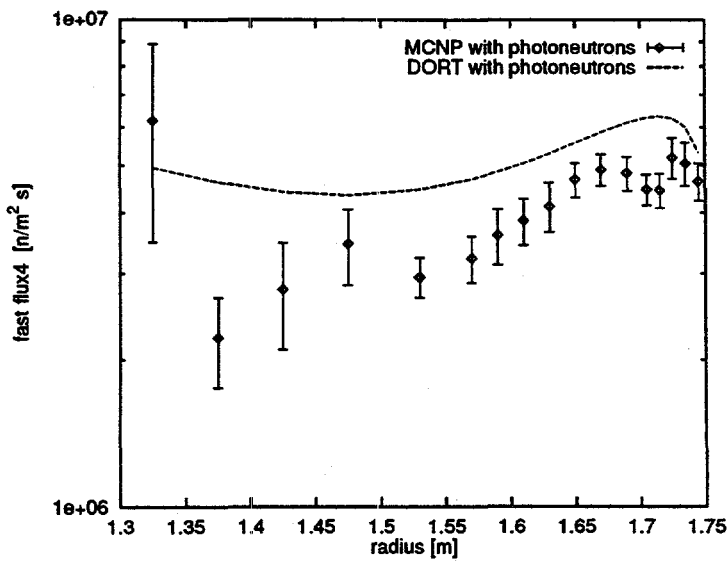


Fig. 4.8. Fast neutron flux ($E = 0.9\text{--}6.43$ MeV) in the heavy water reflector at the outer radial vessel wall calculated with MCNP and DORT including photoneutron production.

5. CONCLUSION

A photoneutron production option was implemented in the MCNP4A code, mainly to supply a tool for reactor shielding calculations in beryllium and heavy water environments of complicated three-dimensional geometries.

Photoneutron production cross sections for deuterium and beryllium were created. Subroutines were developed to calculate the probability of photoneutron production at photon collision sites and the energy and flight direction of the created photoneutrons. These subroutines were implemented into MCNP4A. Some small program changes were necessary for processing the input to read photoneutron production cross sections and to install a photoneutron switch. Some arrays were installed or extended to sample photoneutron creation and loss information, and output routines were changed to give the appropriate summary tables.

To verify and validate the photoneutron production data and the MCNP4A implementations, the yields of photoneutron sources were calculated and compared with experiments. In the case of deuterium-based photoneutron sources, the calculations agreed well with the experiments; the beryllium-based photoneutron source calculations were as much as 30% higher compared with the measurements. More accurate beryllium photoneutron cross sections would be desirable. To apply the developed method to a real shielding problem, the fast neutron fluxes in the heavy water filled reflector vessel of the ANS reactor were investigated and compared against published DORT calculations. Considering the complete independence between the calculations, the 10 to 20% lower fluxes obtained with MCNP4A compared with the DORT results were more than satisfactory, as the discrepancy is based primarily on differences in the calculated thermal neutron fluxes.



6. REFERENCES

1. J. Chadwick and M. Goldhaber, *Nature* **134**, 237 (1934).
2. L. Szillard and T.A. Chalmers, *Nature* **134**, 494 (1934).
3. Ch. Döderlein, "Kinetik und Dynamik eines Forschungsreaktors mit reflektiertem Kom-paktkern," Ph.D. dissertation, Technische Universität München, February 1995.
4. *ANS Conceptual Design Report Summary*, ORNL/TM-12184, Martin Marietta Energy Systems, Inc., Oak Ridge National Laboratory, June 1992.
5. Judith F. Briesmeister, Ed. *MCNP - A General Monte Carlo Code N-particle Transport Code Version 4A*, LA-12625-M, Los Alamos National Laboratory, Los Alamos, New Mexico, 1993.
6. A. O. Hanson, *Radioactive Neutron Sources*, in *Fast Neutron Physics Part I*, Interscience Publishers, Inc., New York, 1960.
7. O. Y. Mafra et al., "Intermediate structure in the Photoneutron and Photofission Cross Sections in U(238) and Th(232)," *Nucl. Phys.* **A186**, 110-126 (1972).
8. E. P. Blizzard and L. S. Abbott, *Reactor Handbook, Vol. III Part B, Shielding*, Interscience Publishers, Inc., New York, 1962.
9. *Reactor Physics Constants*, ANL-5800, Argonne National Laboratory, Chicago, Illinois, July 1963.
10. R. D. Evans, *The Atomic Nucleus*, McGraw-Hill Book Company, New York, 1970.
11. J. Spanier and E. M. Gelbard, *Monte Carlo Principles and Neutron Transport Problems*, Addison-Wesley Publishing Company, London, 1969.
12. L. Hulthen and B. C. H. Nagel, "The Photodisintegration of the Deuteron," *Phys. Rev.* **90**, 62-69 (1953).
13. R. J. Hughes et al., "The Photoneutron Cross Section of Be," *Nucl. Phys.* **A238**, 189-198 (1975).
14. S. I. Warshaw, " 4π Photoneutron Cross Section for Be(9) from Threshold to 16 MeV: Initial Evaluation," Physical Data Note PD-175, Lawrence Livermore National Laboratory, Livermore, California, 1989.
15. R. D. Edge, *Nuclear Physics* **2**, 485 (1956).
16. J. H. Gibbson et al., *Physical Review* **114**, 1319 (1959).
17. W. John and J. M. Prosser, *Physical Review* **127**, 231 (1962).
18. R. Bösch et al., *Helvetica Physica Acta* **36**, 657 (1963).
19. B. L. Berman et al., *Physical Review* **163**, 958 (1967).

20. M. Fujishiro et al., *Canadian Journal of Physics* **60**, 1672 (1982).
21. M. J. Jakobson, "Photodisintegration of Be(9) from Threshold to 5 MeV," *Physical Review* **123**, 229 (1961).
22. S. Costa et al., *Nuovo Cimento* **42B**, 306 (1966).
23. F. Bensch and F. Vesely, "Yields and Spectra of Some Spherical Photo Neutron Sources," *J. Nucl. Ener.* **23**, 537-550 (1969).
24. A. Wattenberg, "Photoneutron Sources and the Energy of the Photoneutrons," *Physical Review* **71**, 497-507 (1947).
25. B. Russel et al., "yields of Photoneutron Sources," *Physical Review* **73**, 545-549 (1948).
26. J. A. Bucholz, *Initial Global 2-D Shielding Analysis for the ANS Core and Reflector*, ORNL/TM-12672, Martin Marietta Energy Systems, Inc., Oak Ridge National Laboratory, June 1995.
27. C. A. Wemple, *Detailed Heatload Calculations for the Conceptual Design of the Advanced Neutron Source Reactor*, ORNL/M-3207, Martin Marietta Energy Systems, Inc., Oak Ridge National Laboratory, December 1993.
28. G. R. Keepin, *Physics of Nuclear Kinetics*, Addison-Wesley Publishing Company, Inc., 1965.
29. B. L. Kirk, *UPDATE: A FORTRAN 77 Source File Manipulator*, ORNL/TDMC-4, Martin Marietta Energy Systems, Inc., Oak Ridge National Laboratory, January 1989.

APPENDIX A. THE MCNP-UPDATE PATCH-FILE



To produce the source of MCNP version 4A with photoneutron production capability, the MCNP4A code file has to be processed with the program UPDATE²⁹ and the following patch. Be aware, that this patch works with IBM-aix workstations only. Modifications in the definition of the arrays have to be made to adjust it to other machines.

```
/*
 ****
 */
/*      <<<< MCNP Version 4a-p >>>>      by Franz Gallmeier      07-28-1995
/*      patch to include photo neutron production
*/
/*      be aware that this patch only works at unix-aix-Systems!!
*/
/* SYSTEMS:
/*      UNICOS:      *define cray,unicos,pointer
/*      CTSS:        *define cray,ctss,pointer,cftlib
#define unix,cheap,aix,pointer
/*      SUN:         *define unix,cheap,sun,pointer
/*      HP:          *define unix,cheap,hpx
/*      ULTRIX:      *define unix,cheap,dec
/*      VMS:         *define vms,cheap
/* GRAPHICS:
/*      CGS:         *define plot,mcplot,gkssim,cgs
#define plot,mcplot,gkssim,xlib
/*      GKS:         *define plot,mcplot
/*      DISSPLA:     *define plot,mcplot,gkssim,disspla,disscgs
/* PARALLEL:
/*      MULT:        *define multt
/*      PVM:         *define multp,pvm
*/
/*
*/
/*
-----changes in comdecks-----comdeck zc
*ident,zc4a-p
*d,zc4a.1
      parameter (kod='mcnp',ver='4a-p')
*/
-----tables
/*
-----charcm
*ident,vv4xe-p
/* ----- add neutron energy group bounaries for febl-array: ebl2(16)
*d,vv4a.1
*d,vv4a.2
      common /tables/ ebl(16),ebln(16),gpt(mipt),qfiss(23),rkt(mtop),
      1 talb(8,2),vco(mcoh),vic(minc),wco(mcoh),
*/
-----add new variables to statically allocated common
/*
-----ident,cm4a-p
/* ----- update length of fixcom: lfixcm= ...+6
*d,cm4a.2
      1 lfixcm=3*mxdt+mink+11*mipt+2*maxv+2*maxf+255+6)
```

```

*/ ----- update length of varcom: nvarcm= ...+32
*d,cm4a.3
    parameter (nvarcm=102*mipt+203+32,1varcm=mipt*(1+8*mxidx)+mcpu+326)
*/
*----- add variables: ineut,npnt,lpna,lpne,lpnz,llpn
*d,cm.36
    4 indt,ink(mink),iphot,ineut,npnt,iplt,ipy(mipt),isb,issw,istrg,
*d,cm4a.14
    5 lpts,lpwb,lrkp,lpna,lpne,lpnz,llpn,
*/
*----- varcom
*----- extend particle production array by energy: febl(2,16) to febl(4,16)
*d,cm.62
    common /varcom/ cpk,cts,dbcn(20),dmp,eacc(4),febl(4,16),osum(3),
*/
*----- tskcom
*----- extend particle production array by energy: febltc(2,16) to febltc(4,16)
*d,cm.173
    1 deb,dti(mlgc),eaccctc(2),eg0,ergace,febltc(4,16),paxtc(6,16,mipt),
*----- update length of tskcom: ntskcm= ...+32
*d,cm4a.70
    parameter (ntskcm=102*mipt+40*mxlv+3*maxf+mlgc+184+32,
*/
*----- dynamical common
*----- fixed dynamical common -----
*----- arrays pna, pne, ipnz and lpn created
*----- storage for neutron production: extend pcc(3,1) to pcc(6,1)
*d,cm.207
    1 eba(mtop,1),pna(1),pne(1),ebd(mtop,1),ebt(mtop,1),
*d,cm4a.75
    6 ksu(1),ipnz(3,1),lpn(1),
*d,cm.232
    1 (kdy,eba),(kdy,pna),(kdy,pne),
*d,cm4a.79
    6 (kdy,ksu),(kdy,ipnz),(kdy,lpn),
*d,cm4a.80
    2 pan(2,6,1),pcc(6,1),pwb(mipt,19,1),rkpl(19,1),shsd(nspt,1),
*/
*----- bd
*ident bd4a-p
*----- adds energybins for photoneutron tally
*i,bd.8
c      energy bins for tally of photon-produced neutrons.
      data ebln/20.,15.,10.,7.,5.,4.,3.,2.,1.5,1.,.6,.3,.1,.05,.01,0./
*/
*----- main---mc
* / STOP for test purposes
* / *ident mc4a-p
* / *i,mc.230
* /      stop
* /
*----- program modifications for input
* / -----comdeck jc
*ident,jc4a-p
* / ----- add one more input card pn, now nkcd=88

```

```

*d,jc4a.1
  parameter (nkcd=87+1,ntalmx=500,mopts=5)
*/ -----ibldat
*ident,ib4a-p
*i,ib4a.7
  data cnm(88),(krq(i,88),i=1,7)/*pn  ',0,0, 0,0, 0, 0,0/
*/ -----pa
*ident im4a-p
*i,pa4a.4
  npnt=0
*/ -----nx
*/ read ineut in nxtit1
*ident nx4a-p
*d,nx.14
  2      9910,9920,9930,600)ica-55
*i,nx.121
  if(nwc.eq.4.and.nqp(2).ne.0)ineut=iitm
*i,nx4a.203
c
c >>>>  photo neutron cross section specification      pn
c
  600 k=0
  l=0
  do 610 i=1,5
  k=k*40+index('abcdefghijklmnopqrstuvwxyz0123456789,',hitm(i:i))+1
  610 l=l*40+index('abcdefghijklmnopqrstuvwxyz0123456789.','
  1 hitm(i+5:i+5))+1
  do 620 m=1,2*mxe1,2
  620 if(kxs(lkxs+m).eq.k.and.kxs(lkxs+m+1).eq.1)return
  if(lfll.lt.lkxs+2*mxe1+5)
  1 call chgmem(mdas,lfll,lkxs+2*mxe1+5005,'nxtit1')
  kxs(lkxs+2*mxe1+1)=k
  kxs(lkxs+2*mxe1+2)=l
  mxe1=mxe1+1
  return
*/ -----stop reading-----ol
*ident,ol4a-p
*d,ol.16
  2      9910,9920,9930,360)ica-55
*i,ol4a.19
c
c >>>>  photo neutron cross section inputs cards      pn
  360  npnt=nwc
  return
*/ -----sd
*ident sd4a-p
*d,sd.43
  lpna=leba+mtop*nee*nmat1
  lpne=lpna+npnt
  lebd=lpne+npnt
*d,sd4a.4

```

```

lipnz=lksu+mxj
llpn=lipnz+3*npnt
lktp=llpn+npnt
*d, sd.148
lpwb=lpcc+6*mxa*kpt(2)
/* -----starts reading card second time (errorhandling)-----ne
*ident,ne4a-p
*d,ne.94
2 9910,9920,9930,640)ica-55
*i,ne4a.65
c
c >>>> photo neutron cross section entry card          pn
640 if(ineut.le.0) call erprnt(2,2,0,0,0,0,1,
1 '54hphys-card entry ineut=0 => no photo neutron production')
      return
c
/* -----read in items second time (feeds dynamical common)-----ny
*ident,ny4a-p
*d,ny4a.1
2 1480,1490,1510,9910,9920,9930,1620)ica-55
*i,ny4a.125
c
c >>>> photo neutron cross section entry card          pn
1620 ht=' '
if(index(htm,'.').eq.0)hitm(nitm+1:nitm+1)='.'
ht(8-index(htm,'.'):10)=hitm
if(ht(8:8).ne.' ' .and.ht(9:9).eq.' ')ht(9:9)='0'
call zaid(1,ht,ipnz(lipnz+1,nwc))
      return
*/
/* -----st
/* add pn card entries to xs-tables
*i,st.108
c
c      add the pn cross sections
do 400 kp=1,npnt
call zaid(2,ht,ipnz(lipnz+1,kp))
ht(10:10)='n'
do 410 i=1,mxe
call zaid(2,hs,ixl(lixl+1,i))
if(hs.eq.ht)go to 400
if(hs(1:6).ne.ht(1:6))go to 410
if(hs(8:9).ne.' ' .and.ht(8:9).ne.' ')go to 410
call erprnt(1,2,0,0,0,0,0,0,
1 '54h//ht// and //hs// are both present on pn card.')
if(hs(8:9).eq.' ')call zaid(1,ht,ixl(lixl+1,i))
      go to 400
410 continue
mxe=mxe+1
call zaid(1,ht,ixl(lixl+1,mxe))
400 continue
*d,st.118

```

```

        mt=index('cdytpmgen',hs(10:10))
*d,st.120
        nt=index('cdytpmgen',ht(10:10))
*-----ix
*d,ix.20
        nt=index('cdytpmgen',ha)
*d,ix.135
        nty(lnty+je)=index('cdytpmgen',ha)
*-----ix
*-----program modifications for cross section processing -----
*-----xa
* *ident,xa4a-p
* *i,xa.52
*c
*c >>>> test STOP
*c      stop 'testing pn-xs processing'
*-----gt
*ident,gt4a-p
*i,gt.16
        ip=0
*d,gt.102
        go to(140,140,140,200,290,310,310,360,500)nty(lnty+ie)
*i,gt.214
c
c >>>> photo neutron cross sections
500 ip=ip+1
        if(ip.gt.npnt) call erprnt(1,2,0,0,0,0,0,0,
        1 '44hgetxst: number of pn-cross sections exceeded')
c
c      set up threshold-energy, nucleus-number and xs-table-number
pne(lpne+ip)=xss(lp+2)
        if(iz(1).ge.1) then
            pna(lpna+ip)=dble(iz(1))
        else
            call erprnt(1,2,0,0,0,0,0,0,
            1 '57hgetxst: pn-atomic-mass of nuclide '//ht// ' lower than 1')
        endif
        lpn(1lpn+ip)=ie
c
c      print information about the table.
        write(iuo,510)ht,nxs(lnxs+1,ie),hk,pna(lpna+ip),pne(lpne+ip),hd
510 format(ix,a10,i8,2x,a70,2f6.1,a10)
*-----ut
* change for extended pcc-array mk*3*mxa*kpt(2) to mk*6*mxa*kpt(2)
*ident,ut4a-p
*d,ut.42
        kpwb=kpcc+mk*6*mxa*kpt(2)+ktask*mip*19*mxa
*-----vt
* change for extended pcc-array j=1,3 to j=1,6
*ident,vt4a-p
*d,vt.10

```

```

do 20 j=1,4
*d,vt.86
do 220 j=1,6
*/ -----cp
*ident cp4a-p
*i,cp4a.3
c
c      photo neutron production
c
if(ineut.ne.0) then
  aa=dble(nint(awn(lawn+lme(1lme+1,m))))
*/
  test
*/
  write(iuo,'("colidp: ineut aa",i4,f8.2)') ineut,aa
  ee=erg
  sw=wgt
  call getpx(aa,ee,px,cs,en)
  call nmaker(aa,ee,px,cs,en)
  wgt=sw
endif
*/ -----eq
*/ --- subroutine summary
*ident eq4a-p
*d,eq.12
  2 'loss to fission','photoneutrons',',',2*' '
*i,eq.216
  if((kpt(1)*kpt(2).ne.0).and.(ineut.ne.0)) call neutp
*/ -----az
*/ --- subroutine action
*ident az4a-p
*d,az.7
  data k1/1,6,13,20/,13/18,19,18/
*d,az.64,az.65
  2 7hfission,6x,7hcapture,6x,7hloss to,6x,7hloss to,6x,6hphoto ,
  3 7x,5htotal/56x,6h(n,xn),6x,7hfission,6x,8hneutrons/)
*/ -----getpx
*addfile,math
*deck xp4a-p
  subroutine getpx(aa,ee,px,cs,en)
c
c      prepares all photoneutron data
c
*call cm
*call jc
  real*8 aa, ee, cs, px
c
c      get xs for energy ee and for nuclide aa if one exists
px=0.0
cs=0.0
en=0.0
if(ee.gt.1.66) then
  do 300 nm=1,npnt

```

```

if((aa.eq.pna(lpna+nn)).and.(ee.gt.pne(lpne+nn))) then
c
c      get cross section data
c
      do 10 i=2,int(xss(jxs(ljxs+1,lpn(llpn+nn))))
         if(ee.le.xss(jxs(ljxs+1,lpn(llpn+nn))+i)) goto 100
10      continue
100     e2=xss(jxs(ljxs+1,lpn(llpn+nn))+i)
         e1=xss(jxs(ljxs+1,lpn(llpn+nn))+i-1)
         de=e2-e1
         s2=xss(jxs(ljxs+2,lpn(llpn+nn))+i-1)
         s1=xss(jxs(ljxs+2,lpn(llpn+nn))+i-2)
         ds=s2-s1
         px=(s1+ds/de*(ee-e1))
         a2=xss(jxs(ljxs+3,lpn(llpn+nn))+i-1)
         a1=xss(jxs(ljxs+3,lpn(llpn+nn))+i-2)
         da=a2-a1
         pa=(a1+da/de*(ee-e1))
*\ isotropic distribution of photoneutron direction if ineut<0
         if(ineut.lt.0) pa=0.0
c
c      calculating photoneutron's relative angle
c      rejection method for chosing cs=cos(theta)
c
         n=0
200     n=n+1
         if(n.gt.100) call erprnt(1,2,0,0,0,0,0,0,
1           '43hgetpx: no angle found after 100 rejections')
         r1=rang()
         r2=rang()
         cs=1.-2.*r1
         f=1.-pa*cs*cs
         if(r2.gt.f) goto 200
c
c      calculate photoneutron energy
c      with equation from ANL-5800 (1963) section 9.7.3
c
         ae=(aa-1.)/aa*(ee-pne(lpne+nn)-ee*ee/1862./(aa-1.))
         be=ee/aa*sqrt(2.*(aa-1.)*(ee-pne(lpne+nn))/931./aa)
         en=ae+be*cs
*/
      test
*/
      write(iuo,'(''getpx: ee px en cs'',4(1pe10.2))')
*/
      &           ee,px,en,cs
      goto 400
      endif
300      continue
      endif
400      continue
      return
      end
*/
-----nmaker

```

```

*deck nm4a-p
  subroutine nmaker(aa,ee,px,cs,en)

c
c      generates a photoneutron
c      and stores it in the particle banck
c
*call cm
*call jc
  if(fiml(1).eq.0..and.kpt(1).ne.0) return
  if(px.gt.0.0) then
c
c      save photon parameters while neutrons are produced.
    npb=npb+1
    do 10 i=1,npb1cm
    10 gpb9cm(npb,i)=gpblcm(i)
    do 20 i=1,lpb1cm
    20 jpb9cm(npb,i)=jpblcm(i)
    do 30 i=1,10*lev
    30 udtr(i)=udt1(i)
    ipt=1
    jgp=0
    npa=1
c
c      make a photoneutron
    ix=15
    pt=rtc(krtc+4,ix)
    t1=wgt*px/pt
    wgt=t1
    erg=en
c
c      transform direction of flight into user system
    call rotas(cs)
c
c      play weight window:
c      find the index of the energy in wwe.
    ic=0
    ib=nww(ipt)
    40 if(ib-ic.eq.1) go to 60
    ih=(ic+ib)/2
    if(erg.lt.wwe(lwwe+ih+mww(ipt))) go to 50
    ic=ih
    go to 40
    50 ib=ih
    go to 40
c
c      bank if weight is within window.
    60 ww=wwf(lwwf+ic1+mxa*(ib-1+mww(ipt)))
    if(ww.eq.0.) go to 80
    if(wgt.lt.ww) go to 70
    goto 200
c

```

```

c      do russian roulette if the weight is below the window.
70      t2=min(wgt*wwp(ipt,3),ww*wwp(ipt,2))
      ii=4
      go to 90
c
c      play weight cutoff game at collisions if required.
80      if(wgt*fiml(1).gt.fiml9(1,1)*wcs2tc(ipt)) goto 200
      t2=wcs1tc(ipt)*fiml9(1,1)/fiml(1)
      ii=6
c
90      if(wgt.lt.t2*rang()) goto 300
      wgt=t2
c
c      bank the new neutron
200      continue
      if(kpt(1).eq.0)go to 300
      paxtc(1,ix,1)=paxtc(1,ix,1)+npa
      paxtc(2,ix,1)=paxtc(2,ix,1)+npa*wgt
      paxtc(3,ix,1)=paxtc(3,ix,1)+npa*wgt*en
      pwb(kpwb+1,ix+3,icl)=pwb(kpwb+1,ix+3,icl)+npa*wgt
      pcc(kpcc+4,icl)=pcc(kpcc+4,icl)+1.
      pcc(kpcc+5,icl)=pcc(kpcc+5,icl)+wgt
      pcc(kpcc+6,icl)=pcc(kpcc+6,icl)+wgt*en
      do 100 i=1,15
100      if(en.gt.ebln(i))go to 110
      febltc(3,i)=febltc(3,i)+1.
      febltc(4,i)=febltc(4,i)+wgt
      vel=slite*sqrt(en*(en+2.*gpt(1)))/(en+gpt(1))
c
c      test
      write(iuo,'(''nmaker: aa ee wgt en cs'',5(1pe10.2))')
      &                               aa,ee,wgt,en,cs
      call bankit(24)
c
c      reset the photon
300      do 310 i=1,lpblcm
310      jpblcm(i)=jpb9cm(npb,i)
      do 320 i=1,npblcm
320      gpblcm(i)=gpb9cm(npb,i)
      do 330 i=1,10*lev
330      udt1(i)=udtr(i)
      npb=npb-1
      endif
      return
      end
*/ ----- ar
/* --- new subroutine neutp modification from subroutine photp
*deck ar4a-p
      subroutine neutp
c      print information about the neutrons produced at photon
c      collisions.

```

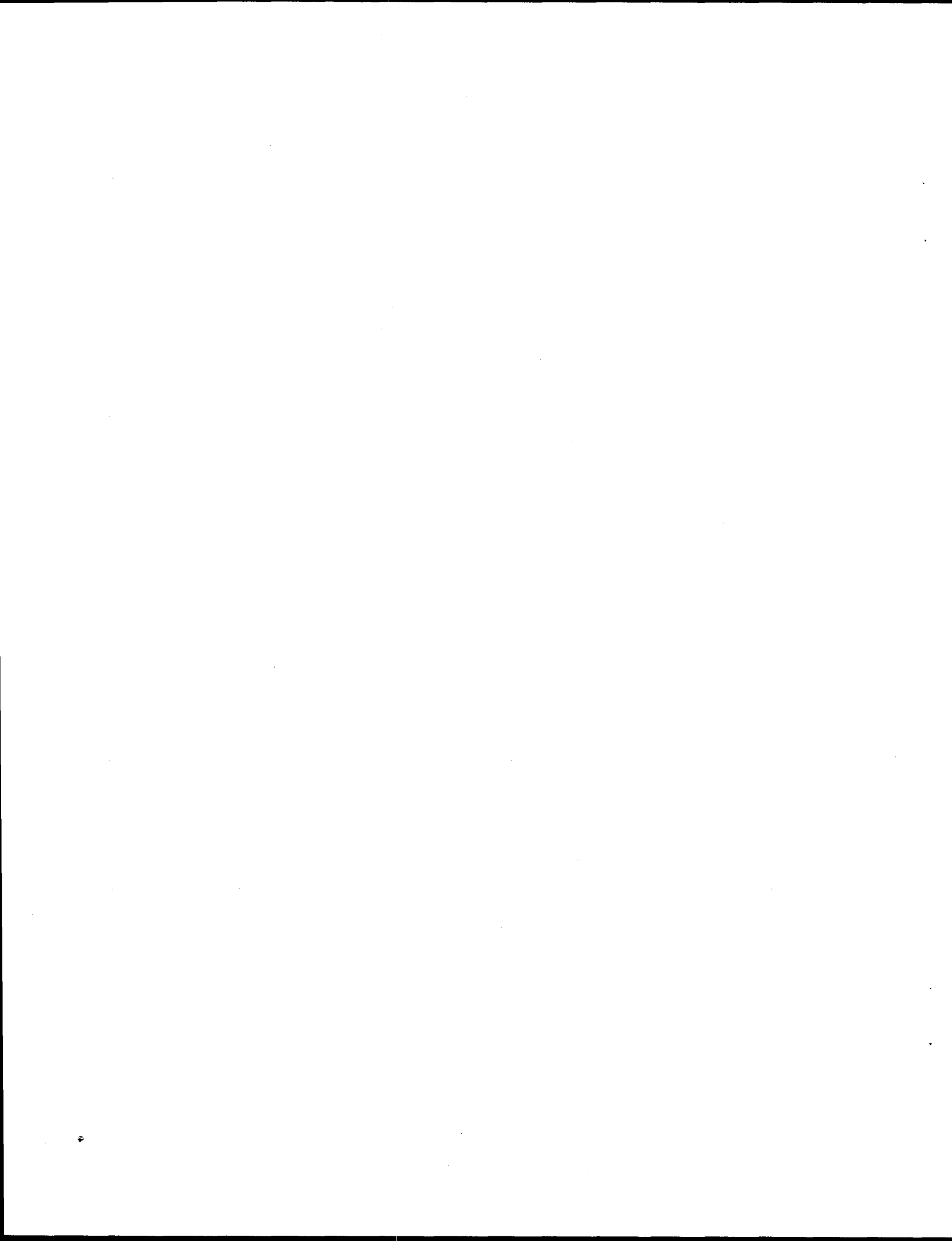
```

*call cm
  character hl(2)*5
  data hl/'  mev','jerks'/
c
  write(iuo,10)
10 format(50h1summary of neutrons produced in photon collisions/)
  if(pax(1,15,1).ne.0.)go to 30
  write(iuo,20)
20 format(/27h no photoneutrons produced.)
  return
c
c      print data for each cell.
30 lw=0
  do 40 i=1,ntal
40 if(jptal(ljpt+2,i).eq.6.and.ktp(lktp+2,i).ne.0.and.
1 jptal(ljpt+4,i).eq.1)lw=1
  write(iuo,50)hl(lw+1)
50 format(8x,4hcell,6x,9hnumber of,6x,10hweight per,5x,10henergy per,
1 5x,11havg neutron,3x,a5,7h/gm per,4x,11hweight/phot,4x,
2 11henergy/phot/19x,8hneutrons,7x,11hsource neut,4x,
3 11hsource neut,
4 6x,6henergy,7x,11hsource neut,5x,9hcollision,6x,9hcollision/)
  do 60 i=1,3
60 tpp(i)=0.
f=1.
  if(lw.eq.1)f=1.60219e-22
  do 80 ic=1,mxa
  t=vol(lvol+ic)*den(lden+ic)
  if(t.eq.0.)t=1.
  t1=0.
  if(pcc(lpcc+5,ic).ne.0.)t1=pcc(lpcc+6,ic)/pcc(lpcc+5,ic)
  t2=1.
  if(pac(lpac+2,4,ic).ne.0.)t2=pac(lpac+2,4,ic)
  do 70 i=1,3
70 tpp(i)=tpp(i)+pcc(lpcc+3+i,ic)
80 write(iuo,90)ic,ncl(lncl+ic),pcc(lpcc+4,ic),fpi*pcc(lpcc+5,ic),
1 fpi*pcc(lpcc+6,ic),t1,f*fpi*pcc(lpcc+6,ic)/t,pcc(lpcc+5,ic)/t2,
2 pcc(lpcc+6,ic)/t2
90 format(2i6,f15.0,t11,1pe18.5,5e15.5)
  t=0.
  if(tpp(2).ne.0.)t=tpp(3)/tpp(2)
  write(iuo,100)tpp(1),fpi*tpp(2),fpi*tpp(3),t
100 format(7x,5htotal,f15.0,t11,1pe18.5,2e15.5)
c
c      print data for each photon energy interval.
  if(mxa.gt.30)write(iuo,110)
110 format(51h1energy distribution of neutrons produced in photon,
1 11h collisions)
  write(iuo,120)
120 format(//2x,6henergy,6x,9hnumber of,8x,6hnumber,7x,10hcum number,
1 6x,9hweight of,7x,6hweight,7x,10hcum weight/9h interval,6x,

```

```
2 8hneutrons,7x,9hfrequency,4x,12hdistribution,6x,8hneutrons,6x,
2 9hfrequency,4x,12hdistribution/1h )
t1=0.
t2=0.
n=16
if(mcal.ne.0)n=jgm(1)
do 130 i=1,n
t1=febl(3,i)/pax(1,15,1)
t2=febl(4,i)/pax(2,15,1)
e=ebln(i)
if(mcal.ne.0)e=xss(jxs(1jxs+1,mgegbt(1))+i-1)
130 write(iuo,140)e,febl(3,i),febl(3,i)/pax(1,15,1),t1,febl(4,i)*fpi,
1 febl(4,i)/pax(2,15,1),t2
140 format(f8.2,f16.0,t11,1pe17.5,4e15.5)
write(iuo,150)pax(1,15,1),1.,pax(2,15,1)*fpi,1.
150 format(/3x,5htotal,f16.0,t11,1pe17.5,e30.5,e15.5)
return
end
```

APPENDIX B. MCNP PHOTONEUTRON CROSS SECTIONS



The program PNMAKE processes the photoneutron cross sections for deuterium and beryllium in MCNP format, which are also enclosed in this Appendix.

```

*****  

c  

c   creates photodisintegration cross sections in MCNP format  

c  

c       for deuterium  

c       calculated with formulas  

c       given by Evans - The Atomic Nucleus  

c  

c       for beryllium  

c       using LANL evaluated data provided in data cards  

c  

*****  

program PNMAKE  

implicit double precision (a-h,o-z)  

real*8 ed(51),eb(51),e(51),xs(51),as(51),a(2)  

integer index(2), ne(2), nd(2), p(2,3)  

character*10 name(2), date, cd  

character*70 desc(2)  

c  

c   energy bins for deuterium photo neutron xsection data  

data ed/  

&   2.225E+00, 2.235E+00, 2.250E+00, 2.270E+00, 2.300E+00  

&   , 2.350E+00, 2.400E+00, 2.500E+00, 2.600E+00, 2.800E+00  

&   , 3.000E+00, 3.200E+00, 3.400E+00, 3.600E+00, 3.800E+00  

&   , 4.000E+00, 4.200E+00, 4.400E+00, 4.600E+00, 4.800E+00  

&   , 5.000E+00, 5.400E+00, 5.800E+00, 6.000E+00, 6.500E+00  

&   , 7.000E+00, 7.500E+00, 8.000E+00, 8.500E+00, 9.000E+00  

&   , 1.000E+01, 1.050E+01, 1.100E+01, 1.150E+01, 1.200E+01  

&   , 1.250E+01, 1.300E+01, 1.350E+01, 1.400E+01, 1.450E+01  

&   , 1.500E+01, 1.550E+01, 1.600E+01, 1.650E+01, 1.700E+01  

&   , 1.750E+01, 1.800E+01, 1.850E+01, 1.900E+01, 1.950E+01  

&   , 2.000E+01/  

c  

c   energy bins for beryllium photo neutron xsection data  

data eb/  

&   1.667E+00, 1.668E+00, 1.673E+00, 1.680E+00, 1.700E+00  

&   , 1.730E+00, 1.780E+00, 1.900E+00, 2.140E+00, 2.240E+00  

&   , 2.430E+00, 2.560E+00, 2.730E+00, 2.820E+00, 2.940E+00  

&   , 3.000E+00, 3.090E+00, 3.200E+00, 3.360E+00, 3.510E+00  

&   , 3.680E+00, 3.870E+00, 4.000E+00, 4.400E+00, 5.400E+00  

&   , 6.200E+00, 6.600E+00, 7.600E+00, 8.100E+00, 9.000E+00  

&   , 1.000E+01, 1.200E+01, 1.400E+01, 1.600E+01, 1.680E+01  

&   , 1.800E+01, 1.900E+01, 2.000E+01, 9.999E+03, 12*9999./  

c  

iu=30  

c  

c   create pn cross section file "pnsets1"  

open(unit=iu,file='pnsets1')

```

```

c
c  pn cross section names and descriptions to be used in MCNP
name(1)='pndeut.01n'
name(2)='pnberyl.01n'
date=' 06/11/95 '
desc(1)='(g,n) data: deuterium (Evans The Atomic nucleus)'
desc(2)='(g,n) data: beryllium (LANL evaluated data)'

c
c  file structure see
index(1)=2          ! atomic number deuterium
index(2)=9          ! atomic number beryllium
a(1)=2.0
a(2)=9.0
ne(1)=51            ! number of energy groups D
ne(2)=38            ! number of energy groups Be
nd(1)=154           ! size of real array= 3*ne+1
nd(2)=115
p(1,1)=1            ! pointer for energy vector \
p(1,2)=53           ! pointer for pn cross section for D
p(1,3)=104          ! pointer for anisotropy factor /
p(2,1)=1            ! pointer for energy vector \
p(2,2)=40           ! pointer for pn cross section for Be
p(2,3)=78           ! pointer for anisotropy factor /
cd='          ,
100 format(a10,f12.6,1pe12.5,1x,a10)
200 format(a70,a10/4(i7,f11.6)/4(i7,f11.6)/4(i7,f11.6)/
1 8i9/8i9/8i9/8i9/8i9/8i9)
300 format(1p,4e20.12)

c
do i=1,1
  aa=a(i)
  do ie=1,ne(i)
    if(a(i).le.2.) then
      e(ie)=ed(ie)
    elseif(a(i).le.9.) then
      e(ie)=eb(ie)
    endif
    ee=e(ie)
    call getpnx(aa,ee,px)
    xs(ie)=px
    call getpna(aa,ee,pa)
    as(ie)=pa
    write(6,'(3(2x,1pe10.4))') e(ie),xs(ie),as(ie)
  enddo
  write(iu,100) name(i), 0.0, 0.0, date
  write(iu,200) desc(i), cd, index(i), fd, (0,0.0,j=2,16),
&           nd(i), (0,j=2,16), (p(i,j),j=1,3),
&           (0,j=4,32)
  write(iu,300) float(ne(i)),(e(j),j=1,ne(i)),
&           (xs(j),j=1,ne(i)),(as(j),j=1,ne(i))
  enddo

```

```

write(6,(''***** pnmake finished *****''))
end

c
c*****subroutine getpna(aa,ee,cs)
c*****implicit double precision (a-h,o-z)
c*****real*8 aa, cs, ee, mm, mp, mn
c
c      subroutine getpna(aa,ee,cs)
      implicit double precision (a-h,o-z)
      real*8 aa, cs, ee, mm, mp, mn
c
c      get b/a+b
c
      cs=0.0
      a=1.0
      b=0.0
      if(aa.eq.2.) then ! Using Evans "The atomic Nucleus" 1970 eq 4.22
         bb=2.225          ! threshold energy for photo neutron production
         hc=1.9733e-11      ! h_bar*c in MeV*cm
         mm=939.57/2.        ! half neutron mass in MeV/c**2
         ro=4.31e-13         ! classical deuterium radius in cm
         mp=2.79             ! mag dipole moment of proton in bohr-magnetons
         mn=-1.91             ! mag dipole moment of neutron in bohr-magneton
         ar=5.5               ! singulet scattering length in units of ro
         rd=0.394              ! effective range of triplet force in units of
         co=2./3./4./137.*(mp-mm)**2 *(hc/2./mm)**2 *1.e24*1.e3
         a=co *sqrt(bb*(ee-bb)) /ee*(1.-ar)**2 *bb
         &                   /(bb+ar*ar*(ee-bb)/2.)
         b=ro*ro/137./(1.-rd)*(sqrt(bb*(ee-bb))/ee)**3 *1.e24*1.e3
      else if(aa.eq.9.) then ! using Jakobson Phys.Rev 123-1 p229 (1961)
         a=1.0
         b=0.0
         if((ee.ge.2.6).and.(ee.lt.3.2)) b=1.0
      else
         goto 1000
      endif
c
      c=a+b
      if(c.le.0.) c=1.0
      cs=b/c
1000  continue
      return
      end

c*****subroutine getpnx(aa,ee,px)
c*****implicit double precision (a-h,o-z)
c*****real*8 aa, ee, px
c*****real*8 eb(50), sb(50)
c
c      energy bins for beryllium photo neutron xsection data
      data eb/
      &      1.666E+00, 1.668E+00, 1.673E+00, 1.680E+00, 1.700E+00

```

```

& , 1.730E+00, 1.780E+00, 1.900E+00, 2.140E+00, 2.240E+00
& , 2.430E+00, 2.560E+00, 2.730E+00, 2.820E+00, 2.940E+00
& , 3.000E+00, 3.090E+00, 3.200E+00, 3.360E+00, 3.510E+00
& , 3.680E+00, 3.870E+00, 4.000E+00, 4.400E+00, 5.400E+00
& , 6.200E+00, 6.600E+00, 7.600E+00, 8.100E+00, 9.000E+00
& , 1.000E+01, 1.200E+01, 1.400E+01, 1.600E+01, 1.680E+01
& , 1.800E+01, 1.900E+01, 2.000E+01, 9.999E+03, 11*9999./

c
c      beryllium photo neutron xsection data in mbarn
data sb/
& 1.000E-04, 1.200E+00, 1.600E+00, 1.450E+00, 1.300E+00
& , 1.100E+00, 8.000E-01, 4.000E-01, 2.900E-01, 2.630E-01
& , 4.050E-01, 4.660E-01, 6.080E-01, 9.810E-01, 1.578E+00
& , 1.332E+00, 6.360E-01, 3.400E-01, 3.510E-01, 2.520E-01
& , 1.870E-01, 3.350E-01, 3.290E-01, 2.000E-01, 8.200E-01
& , 1.140E+00, 1.500E+00, 1.520E+00, 1.380E+00, 1.580E+00
& , 1.400E+00, 1.200E+00, 8.000E-01, 5.000E-01, 4.000E-01
& , 6.000E-01, 1.300E+00, 1.850E+00, 9.999E+03, 11*9999./

c
c      get xs for energy ee
c
ed=2.2245
if((aa.eq.2.).and.(ee.gt.ed)) then
  px=phopde(ee)
else if(aa.eq.9..and.ee.gt.eb(1)) then
  do 20 i=2,39
    if(ee.le.eb(i)) goto 200
20  continue
200 ds=sb(i)-sb(i-1)
  de=eb(i)-eb(i-1)
  px=(sb(i-1)+ds/de*(ee-eb(i-1)))*1.e-3
else
  px=0.0
endif
return
end
*****
c
c      double precision function phopde(ee)
c      implicit double precision (a-h,o-z)
c      real*8 ee,pi,bb,mm,ro,mp,mn,ar,rd,co,a,b
c
pi=3.1515926      ! Pi
bb=2.225          ! threshold energy for photo neutron production
hc=1.9733e-11     ! h_bar*c in MeV*cm
mm=939.57/2.       ! half neutron mass in MeV/c**2
ro=4.31e-13        ! classical deuterium radius in cm
mp=2.79            ! mag dipole moment of proton in bohr-magneton
mn=-1.91           ! mag dipole moment of neutron in bohr-magneton
ar=5.5             ! singulet scattering length in units of ro
rd=0.394           ! effective range of triplet force in units of

```

```
co=2./3.*pi/137.* (mp-mm)**2 *(hc/2./mm)**2 *1.e24*1.e3
c
if(ee.gt.2.225)then
  a=co *sqrt(bb*(ee-bb)) /ee*(1.-ar)**2 *bb
  &                               /(bb+ar*ar*(ee-bb)/2.)
  b=8.*pi/3.*ro*ro/137./(1.-rd)*(sqrt(bb*(ee-bb))
  &                               /ee)**3 *1.e24*1.e3
else
  a=0.0
  b=0.0
endif
c
phopde=(a+b)*1.e-3
return
end
c
*****
```

pndeut.01n .000000 0.00000E+00 06/11/95
 (g,n) data: deuterium (Evans The Atomic nucleus)

2	.000000	0	.000000	0	.000000	0	.000000
0	.000000	0	.000000	0	.000000	0	.000000
0	.000000	0	.000000	0	.000000	0	.000000
0	.000000	0	.000000	0	.000000	0	.000000
154	0	0	0	0	0	0	0
0	0	0	0	0	0	0	0
1	53	104	0	0	0	0	0
0	0	0	0	0	0	0	0
0	0	0	0	0	0	0	0
0	0	0	0	0	0	0	0
5.1000000000000E+01	2.224999904633E+00	2.234999895096E+00	2.2500000000000E+00				
2.269999980927E+00	2.299999952316E+00	2.349999904633E+00	2.400000095367E+00				
2.5000000000000E+00	2.599999904633E+00	2.799999952316E+00	3.0000000000000E+00				
3.200000047684E+00	3.400000095367E+00	3.599999904633E+00	3.799999952316E+00				
4.0000000000000E+00	4.199999809265E+00	4.400000095367E+00	4.599999904633E+00				
4.800000190735E+00	5.0000000000000E+00	5.400000095367E+00	5.800000190735E+00				
6.0000000000000E+00	6.5000000000000E+00	7.0000000000000E+00	7.5000000000000E+00				
8.0000000000000E+00	8.5000000000000E+00	9.0000000000000E+00	1.0000000000000E+01				
1.0500000000000E+01	1.1000000000000E+01	1.1500000000000E+01	1.2000000000000E+01				
1.2500000000000E+01	1.3000000000000E+01	1.3500000000000E+01	1.4000000000000E+01				
1.4500000000000E+01	1.5000000000000E+01	1.5500000000000E+01	1.6000000000000E+01				
1.6500000000000E+01	1.7000000000000E+01	1.7500000000000E+01	1.8000000000000E+01				
1.8500000000000E+01	1.9000000000000E+01	1.9500000000000E+01	2.0000000000000E+01				
0.0000000000000E+00	1.946903953439E-04	2.927739953118E-04	3.739331325916E-04				
4.613213289787E-04	5.796526794417E-04	6.898193568887E-04	9.059822868087E-04				
1.114957245937E-03	1.488627424596E-03	1.788352056263E-03	2.016225204836E-03				
2.182556028574E-03	2.298851628205E-03	2.375489111539E-03	2.421132284826E-03				
2.442769139018E-03	2.445941457135E-03	2.435007145944E-03	2.413379309511E-03				
2.383726575216E-03	2.308230504882E-03	2.220302152672E-03	2.174045780053E-03				
2.056482364803E-03	1.940657685862E-03	1.829778150944E-03	1.725340663008E-03				
1.627889742952E-03	1.537445327242E-03	1.376395675456E-03	1.304932004227E-03				
1.238884506544E-03	1.177793772893E-03	1.121225960606E-03	1.068778952312E-03				
1.020084376090E-03	9.748072715952E-04	9.326444760585E-04	8.933223745318E-04				
8.565943971960E-04	8.222384865905E-04	7.900546597500E-04	7.598627305300E-04				
7.315002213339E-04	7.048204720394E-04	6.796909416062E-04	6.559916911588E-04				
6.336140340926E-04	6.124593375924E-04	5.924379600131E-04	0.000000000000E+00				
4.245981903305E-02	1.070052875179E-01	1.912851146353E-01	3.074625328211E-01				
4.647682499701E-01	5.797858073846E-01	7.236438680411E-01	8.032821458660E-01				
8.818913874127E-01	9.179985859795E-01	9.377461481541E-01	9.498656446328E-01				
9.579264384795E-01	9.636127658272E-01	9.678076187839E-01	9.710126090516E-01				
9.735312300705E-01	9.755566302550E-01	9.772169914457E-01	9.786003667567E-01				
9.807683447791E-01	9.823845929647E-01	9.830464665630E-01	9.843954578779E-01				
9.854280834258E-01	9.862426167226E-01	9.869007833179E-01	9.874432048246E-01				
9.878976566493E-01	9.886156953803E-01	9.889040597011E-01	9.891568345037E-01				
9.893801825457E-01	9.895789285285E-01	9.897569020984E-01	9.899171808223E-01				
9.900622655021E-01	9.901942087776E-01	9.903147108865E-01	9.904251919429E-01				
9.905268471738E-01	9.906206896139E-01	9.907075834525E-01	9.907882703316E-01				
9.908633902708E-01	9.909334984555E-01	9.909990788100E-01	9.910605550506E-01				
9.911182997474E-01	9.911726417996E-01						

pnbery.01n .000000 0.00000E+00 06/05/95
 (g,n) data: beryllium (LANL evaluated data)

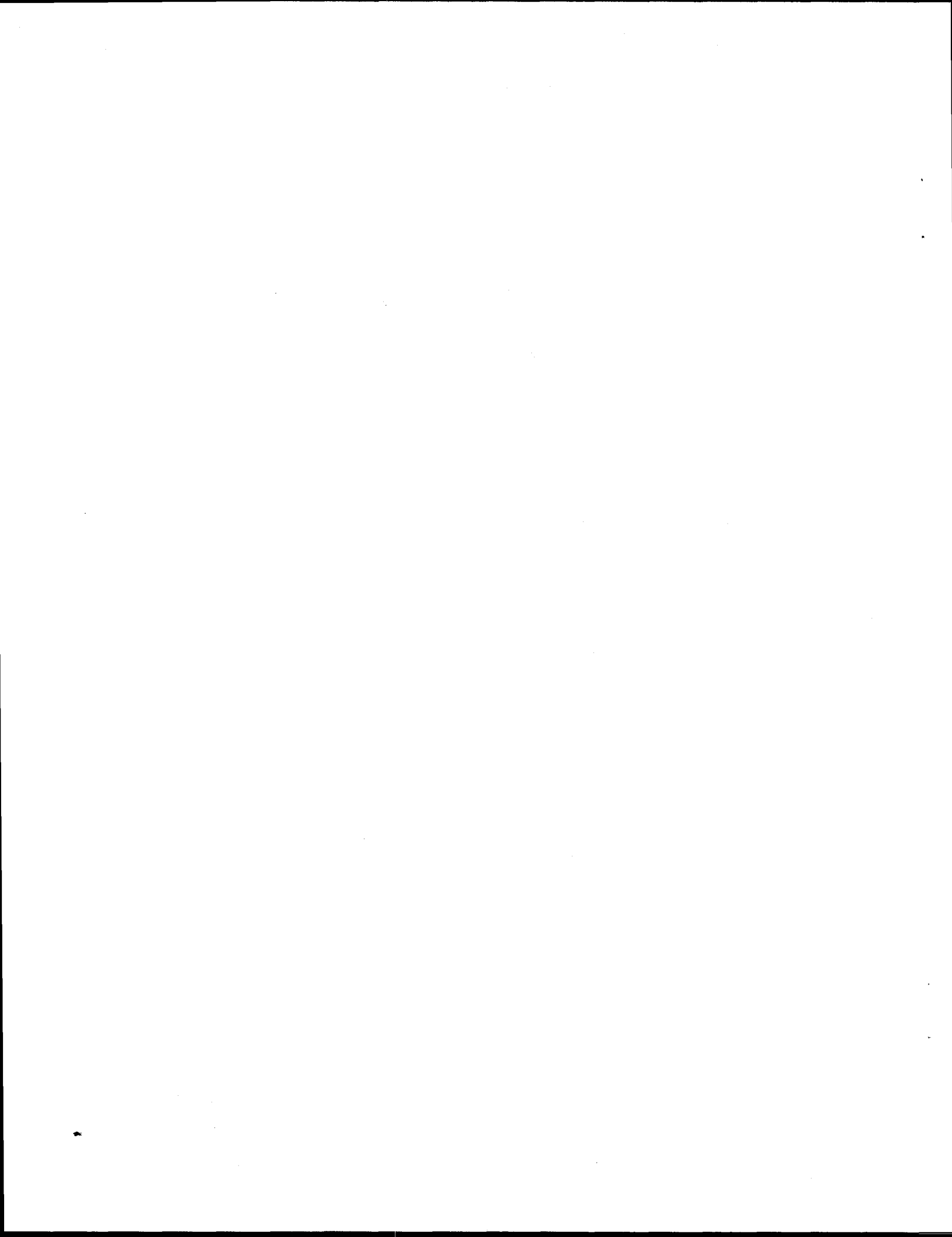
9	.000000	0	.000000	0	.000000	0	.000000
0	.000000	0	.000000	0	.000000	0	.000000
0	.000000	0	.000000	0	.000000	0	.000000
0	.000000	0	.000000	0	.000000	0	.000000
115	0	0	0	0	0	0	0
0	0	0	0	0	0	0	0
1	40	78	0	0	0	0	0
0	0	0	0	0	0	0	0
0	0	0	0	0	0	0	0
0	0	0	0	0	0	0	0
3.800000000000E+01	1.667000055313E+00	1.667999982834E+00	1.672999978065E+00				
1.679999947548E+00	1.700000047684E+00	1.730000019073E+00	1.779999971390E+00				
1.899999976158E+00	2.140000104904E+00	2.24000009537E+00	2.430000066757E+00				
2.559999942780E+00	2.73000019073E+00	2.819999933243E+00	2.940000057220E+00				
3.000000000000E+00	3.089999914169E+00	3.200000047684E+00	3.359999895096E+00				
3.509999990463E+00	3.68000066757E+00	3.869999885559E+00	4.000000000000E+00				
4.400000095367E+00	5.40000095367E+00	6.199999809265E+00	6.599999904633E+00				
7.599999904633E+00	8.10000381470E+00	9.000000000000E+00	1.000000000000E+01				
1.200000000000E+01	1.400000000000E+01	1.600000000000E+01	1.679999923706E+01				
1.800000000000E+01	1.900000000000E+01	2.000000000000E+01	6.000858126116E-04				
1.200000104681E-03	1.60000099838E-03	1.450000116555E-03	1.30000014063E-03				
1.10000076089E-03	8.000000499189E-04	4.000000249594E-04	2.90000054296E-04				
2.63000239359E-04	4.050000204286E-04	4.660000128355E-04	6.08000093281E-04				
9.810000527939E-04	1.578000024406E-03	1.332000080433E-03	6.36000077970E-04				
3.400000197254E-04	3.510000276389E-04	2.520000160225E-04	1.870000153193E-04				
3.350000242563E-04	3.290000118120E-04	2.000000124797E-04	8.200000317954E-04				
1.14000039842E-03	1.50000071246E-03	1.52000053123E-03	1.38000060778E-03				
1.580000117961E-03	1.40000042655E-03	1.200000104681E-03	8.00000499189E-04				
5.000000237487E-04	4.000000249594E-04	6.000000523403E-04	1.30000014063E-03				
1.850000111712E-03	0.000000000000E+00	0.000000000000E+00	0.000000000000E+00				
0.000000000000E+00	0.000000000000E+00	0.000000000000E+00	0.000000000000E+00				
0.000000000000E+00	0.000000000000E+00	0.000000000000E+00	0.000000000000E+00				
0.000000000000E+00	5.000000000000E-01	5.000000000000E-01	5.000000000000E-01				
5.000000000000E-01	5.000000000000E-01	0.000000000000E+00	0.000000000000E+00				
0.000000000000E+00	0.000000000000E+00	0.000000000000E+00	0.000000000000E+00				
0.000000000000E+00	0.000000000000E+00	0.000000000000E+00	0.000000000000E+00				
0.000000000000E+00	0.000000000000E+00	0.000000000000E+00	0.000000000000E+00				
0.000000000000E+00	0.000000000000E+00	0.000000000000E+00	0.000000000000E+00				

pndeut.02n .000000 0.00000E+00 06/11/95

(g,n) data: deuterium (Keepin-digitalized)

2	.000000	0	.000000	0	.000000	0	.000000
0	.000000	0	.000000	0	.000000	0	.000000
0	.000000	0	.000000	0	.000000	0	.000000
0	.000000	0	.000000	0	.000000	0	.000000
133	0	0	0	0	0	0	0
0	0	0	0	0	0	0	0
1	46	90	0	0	0	0	0
0	0	0	0	0	0	0	0
0	0	0	0	0	0	0	0
0	0	0	0	0	0	0	0
4.4000000000000E+01	2.224999904633E+00	2.236000061035E+00	2.269999980927E+00				
2.336999893188E+00	2.411000013351E+00	2.539000034332E+00	2.674000024796E+00				
3.012000083923E+00	3.348999977112E+00	3.686000108719E+00	4.022999763489E+00				
4.360000133514E+00	4.697999954224E+00	5.034999847412E+00	5.372000217438E+00				
5.709000110626E+00	6.046999931335E+00	6.383999824524E+00	6.721000194550E+00				
7.058000087738E+00	7.395999908447E+00	8.069999694824E+00	8.744000434875E+00				
9.418999671936E+00	1.009000015259E+01	1.077000045776E+01	1.143999958038E+01				
1.211999988556E+01	1.244999980927E+01	1.3000000000000E+01	1.3500000000000E+01				
1.4000000000000E+01	1.4500000000000E+01	1.5000000000000E+01	1.5500000000000E+01				
1.6000000000000E+01	1.6500000000000E+01	1.7000000000000E+01	1.7500000000000E+01				
1.8000000000000E+01	1.8500000000000E+01	1.9000000000000E+01	1.9500000000000E+01				
2.0000000000000E+01	0.0000000000000E+00	2.627000039422E-04	5.254000078844E-04				
7.881000416289E-04	1.051000048966E-03	1.313000026125E-03	1.524000121024E-03				
1.857000081527E-03	2.062000134179E-03	2.180000170302E-03	2.259000170239E-03				
2.285000194362E-03	2.272000182301E-03	2.259000170239E-03	2.207000121993E-03				
2.154000146179E-03	2.102000097932E-03	2.040999986316E-03	1.983000134242E-03				
1.920000048280E-03	1.857000081527E-03	1.734000049936E-03	1.602000074184E-03				
1.487000059185E-03	1.379000014001E-03	1.282000006532E-03	1.174000080558E-03				
1.082000068558E-03	1.040000011250E-03	1.018000055028E-03	9.724000558186E-04				
9.329000558498E-04	8.911000317392E-04	8.544000196964E-04	8.201000483940E-04				
7.880000250302E-04	7.579000356168E-04	7.296000469565E-04	7.030000424506E-04				
6.779000485064E-04	6.543000055191E-04	6.320000591055E-04	6.108000568587E-04				
5.909000319763E-04	0.000000000000E+00	4.675133477329E-02	1.912851146353E-01				
4.282889599032E-01	6.004375039951E-01	7.599933492165E-01	8.407008796948E-01				
9.195146200041E-01	9.472564472704E-01	9.605989716545E-01	9.682194970706E-01				
9.730720017793E-01	9.764096178852E-01	9.788189240234E-01	9.806372960066E-01				
9.820543791775E-01	9.831905226275E-01	9.841153331994E-01	9.848839634068E-01				
9.855323233007E-01	9.860877347524E-01	9.869829446509E-01	9.876746003610E-01				
9.882251971580E-01	9.886705566793E-01	9.890445497227E-01	9.893547643509E-01				
9.896234095956E-01	9.897399467130E-01	9.899171808223E-01	9.900622655021E-01				
9.901942087776E-01	9.903147108865E-01	9.904251919429E-01	9.905268471738E-01				
9.906206896139E-01	9.907075834525E-01	9.907882703316E-01	9.908633902708E-01				
9.909334984555E-01	9.909990788100E-01	9.910605550506E-01	9.911182997474E-01				
9.911726417996E-01							

APPENDIX C. MCNP INPUT FOR THE PHOTONEUTRON SOURCE CALCULATIONS



This appendix contains the MCNP4A input file for the photoneutron source calculations described in Sect. 4.1. Different source-target combinations can be chosen.

```

message: outp=pnsben.o srctp=pnsben.s runtpe=pnsben.r mctal=pnsben.m

        bensch photoneutron source Sb-Be
c -----
c (uses Iodine-xs instead of Sb)
c
c cells:
c -----
1 8 0.0790      -1
2 7 0.0330      -2 +1
3 6 0.1236      -3 +2
4 6 0.1236      -4 +3
5 6 0.1236      -5 +4
6 0           -6 +5

c surfaces:
c -----
1 so 0.50
2 so 0.51
3 so 1.00
4 so 1.60
5 so 2.50
6 so 5.00

c
c peripheral cards:
c -----
mode n p
nps 500000
phys:p 0.01 1 0 1
cut:p 1e5 1.5 -0.5 -0.25 1.0
print 130
c
c materials:
c -----
c natural Gallium
m1 31000.50c 1.00
c Indium115 mason2
m2 49115.60c 1.00
c NaF
m3 11023.50c 0.50 9019.50c 0.50
c La203 (La140)
m4 57140.60c 0.40 8016.50c 0.60
c D20
m5 1002.55c 0.667 8016.50c 0.333
c Beryllium
m6 4009.50c 1.00
c tin

```

```
m7      50000.35c 1.00
c      iodine as substitute for antimony
m8      53127.60c 1.00
c      manganese
m9      25055.50c 1.00
c
c      photo neutron production cross sections:
c      -----
pn      pndeut.01n  pnbery.01n
c
c      weight window setting with importances:
c      -----
imp:n  1 1 1 1 1 0
imp:p  1 1 1 1 1 0
wwp:n  5 3.0 5 0 0.01
wwp:p  5 3.0 5 0 0.1
c
c      source definition cards:
c      -----
sdef   erg=d1 pos=0 0 0 rad=d2 cel=1 par=2
si2    0.0 0.5
sp2    -21 2
c      sc1      Gallium
c      si1      1 1.8611 2.1095 2.2017 2.4910 2.5078
c      sp1      d 0.0520 0.0100 0.2611 0.0750 0.1282
c      sc1      NaF
c      si1      1 2.7541
c      sp1      d 1.00
c      sc1      La203
c      si1      1 2.5217
c      sp1      d 1.00
c      sc1      In
c      si1      1 1.7524 2.1123
c      sp1      d 0.0239 0.1538
sc1    Sb
si1    1 1.6910 2.0910
sp1    d 0.4900 0.0573
c      sc1      Mn
c      si1      1 1.8107 2.1131 2.5229 2.6575 2.9598 3.3696
c      sp1      d 0.2719 0.1434 0.0099 0.0065 0.0031 0.0017
c
c      tally:
c      -----
f1:n   5
```

INTERNAL DISTRIBUTION

1. J. A. Bucholz	16. B. A. Worley
2-6. F. X. Gallmeier	17. C. D. West
7. D. T. Ingersoll	18. ORNL Patent Office
8-11. R. L. Johnson	19. Central Research Library
12. T. J. McManamy	20. Document Reference Section
13. J. V. Pace III	21. Y-12 Technical Library
14. D. L. Selby	22-23. Laboratory Records Department
15. C. O. Slater	24. Laboratory Records (RC)

EXTERNAL DISTRIBUTION

25. D. D. Carlson, U.S. Nuclear Regulatory Commission, T10G6, Washington, DC 20555
26. U.S. Department of Energy, Oak Ridge Operations, FEDC, MS 8218, P.O. Box 2009, Oak Ridge, TN 37831-8218
27-28. Office of Scientific and Technical Information, P.O. Box 62, Oak Ridge, TN 37831